Progress in Biomedical Engineering

PURPOSE-LED PUBLISHING™

ACCEPTED MANUSCRIPT • OPEN ACCESS

Advancing Physical Activity Monitoring through Bioimpedance Measurement: A Review

To cite this article before publication: Ifeanyi Jacobs *et al* 2026 *Prog. Biomed. Eng.* in press https://doi.org/10.1088/2516-1091/ae3671

Manuscript version: Accepted Manuscript

Accepted Manuscript is "the version of the article accepted for publication including all changes made as a result of the peer review process, and which may also include the addition to the article by IOP Publishing of a header, an article ID, a cover sheet and/or an 'Accepted Manuscript' watermark, but excluding any other editing, typesetting or other changes made by IOP Publishing and/or its licensors"

This Accepted Manuscript is **© 2026 The Author(s). Published by IOP Publishing Ltd**.

As the Version of Record of this article is going to be / has been published on a gold open access basis under a CC BY 4.0 licence, this Accepted Manuscript is available for reuse under a CC BY 4.0 licence immediately.

Everyone is permitted to use all or part of the original content in this article, provided that they adhere to all the terms of the licence https://creativecommons.org/licences/by/4.0

Although reasonable endeavours have been taken to obtain all necessary permissions from third parties to include their copyrighted content within this article, their full citation and copyright line may not be present in this Accepted Manuscript version. Before using any content from this article, please refer to the Version of Record on IOPscience once published for full citation and copyright details, as permissions may be required. All third party content is fully copyright protected and is not published on a gold open access basis under a CC BY licence, unless that is specifically stated in the figure caption in the Version of Record.

View the article online for updates and enhancements.

This content was downloaded from IP address 156.62.3.21 on 19/01/2026 at 22:40

Advancing Physical Activity Monitoring through Bioimpedance Measurement: A Review

Ifeanyi Jacobs [a, *, c], Andrew Lowe [a], Lorenzo Garcia [a, b], Huiyang Zhang [a]

[a] Institute of Biomedical Technologies, Auckland University of Technology, Auckland 1010, New Zealand
[b] Biomechanical Design Lab, Auckland University of Technology, Auckland 1010, New Zealand
[c] Department of Mechanical Engineering, University of Nigeria Nsukka
∗ Author to whom any correspondence should be addressed.

Abstract

Bioimpedance measurements have gained significant attention due to their ability to assess body composition, muscle health, and internal physiological states without the need for intrusive procedures. This review paper explores the advancements and applications of bioimpedance technology, a non-invasive and cost-effective method for real-time monitoring of physiological parameters and physical activities. It discusses key measurement modalities such as bioelectrical impedance analysis (BIA), electrical impedance myography (EIM), and electrical impedance tomography (EIT), highlighting their unique advantages and applications. It also examines the role of biopotential electrodes, both polarizable and non-polarizable, in ensuring accurate physiological measurements. Despite challenges such as low spatial resolution, motion artifacts and sensitivity to electrode placement, the review highlights promising solutions. These include the integration of hybrid sensor systems, machine learning algorithms for signal interpretation, and the development of wearable and flexible electronics. The paper concludes by emphasizing the growing potential of bioimpedance technology in fields such as sports science, rehabilitation, personalized healthcare, fitness monitoring, and human-machine interaction, suggesting a future where continuous physiological monitoring becomes seamlessly embedded in daily life.

Keywords: physical activity, bioimpedance measurement, muscle activity, biopotential electrode, gesture recognition, wearable systems.

1. Introduction

Physical activity is essential for maintaining health and preventing various chronic diseases. It involves any bodily movement (e.g. walking or running) produced by skeletal muscles that requires energy expenditure [1], [2]. In recent years, the evaluation of physical activity has evolved significantly from subjective (e.g. self-report questionnaires) [3] to objective (e.g. sensor-based) [4] measures, leveraging advancements in technology to provide more comprehensive insights into health, fitness and human behaviour. Human Activity Recognition (HAR) is a technique for automatically identifying and classifying physical activities performed by individuals using data from various sensors and machine learning models [5], [6], [7]. It is a rapidly evolving field with applications in healthcare and well-being, smart homes and ambient assisted living, intelligent surveillance systems, fitness and sports, workplace safety and interactive gaming entertainment [8], [9].

*Corresponding Author: Ifeanyi Jacobs
Email: Ifeanyi.jacobs@autuni.ac.nz

Accepted Manuscript

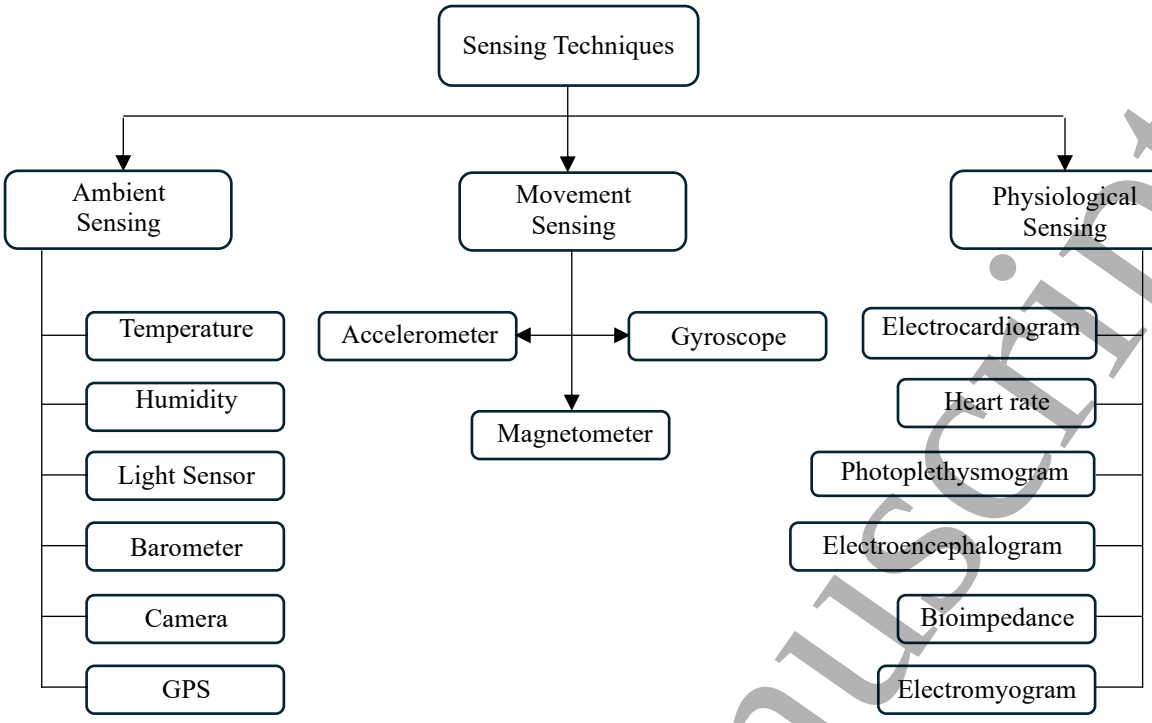

Fig.1: Classification of Sensing Techniques in HAR

Sensing techniques in HAR can be broadly classified into ambient, movement, and physiological sensing as shown in figure 1 [8]. These sensors possess characteristics such as sensitivity, accuracy, range, resolution, and precision [10]. Ambient sensors are sensing devices employed to monitor various environmental parameters such as motion, light, temperature, pressure and humidity. However, they can provide important information about an individuals' context and interaction with their surrounding environment [11]. Movement sensors, also referred as inertia measurement units (IMUs) measure the acceleration, angular velocity and surrounding magnetic field respectively [12], [13]. However, they are embedded in smartphones [14], [15] and wearable devices [16] to capture body's motion data in 3-D (x, y, and z axis) [17]. Physiological sensors are sensing devices that detect, measure, and monitor biological signals from the human body [18], [19]. They are used in healthcare, sports science, and human-computer interaction applications [20]. Several wearable devices and smartphones are integrated with these sensors to monitor biological signals, which makes them non-invasive and easy to use [10]. The data obtained from these sensing techniques have the potential to detect, recognize, and monitor human activities in real time [21], [22]. Several studies have presented comprehensive surveys of HAR using machine learning algorithms and techniques as shown in table 1.

Table 1: Summary of Previous Surveys on Human Activity Recognition

Ref	Aim	Contributions/Highlights	Research Gaps
[8]	To provide a comprehensive survey of HAR techniques that utilize inertial,	• Discusses the integration of sensors into wearable devices like smartphones and smartwatches. • Compares the performance of classical machine learning (CML) and DL models,	• Need for standardized methodologies that can generalize to a diverse set of activities performed by different subjects.

Accepted Manuscript

	physiological, and environmental sensors.	showing that while DL models achieve high accuracy. • Discusses various preprocessing techniques and feature extraction methods used in HAR and their importance.	• Need to combine data from multiple sensors to improve the reliability and accuracy of HAR systems. • Lack of HAR models that can be executed directly on wearable devices.
[23]	To investigate and review the optimal machine learning algorithms and techniques for HAR across various application domains	• Highlights the strengths and weaknesses of vison based and non-vision-based methods. • Categorizes human activities into four major types: composite, concurrent, sequential, and interleaved activities. • Analyses various machine learning techniques used in HAR, including traditional methods, deep learning, and ensemble learning.	• Difficulty in recognizing complex and dynamic activities involving multiple actions in varied situations. • Privacy issues in vision-based HAR techniques due to constant observation and recording. • Lack of research to determine the best machine learning algorithms and sensors for specific HAR applications
[24]	To systematically review and classify multi-sensor fusion methods for HAR	• Organizes fusion methods into data-level, feature-level, decision-level and mixed fusion. • Mixed fusion methods often outperform single fusion methods. • Suggests that multi-sensor fusion improves recognition accuracy • Effectiveness of fusion methods is dependent on dataset characteristics.	• Lack of justification for choosing specific fusion methods for given datasets. • Limited studies on combining manual and automatic feature extraction. • Limited exploration of fusion methods in medical scenarios.
[25]	To provide a comprehensive review of data fusion and multiple classifier system techniques for HAR, with an emphasis on mobile and wearable devices	• Summarizes recent advancements in data fusion, feature fusion, and multiple classifier systems for HAR, covering methods, sensor modalities, and applications. • Provides a structured taxonomy of fusion and classifier strategies, analysing their strengths, weaknesses, and suitability for health monitoring. • Integrates diverse sensor modalities and classifier outputs to enhance the accuracy of HAR.	• Limited studies on optimal sensor combinations, handling non-linear data, and real-time fusion • Lack of hybrid approaches combining handcrafted and deep learning (DL) features fusion. • Privacy concerns with vision-based sensors, energy efficiency, and scalability for real-time applications.
[26]	To provide a comprehensive overview on the current state of electrical impedance myography (EIM) technology and its application in sports health.	• Categorizes electrodes into wet and dry types, with a focus on flexible electrodes for wearable monitoring. • Introduces multi-frequency EIM for comprehensive muscle impedance measurement. • Reviews data processing methods, including machine learning techniques. • Highlights finite element modelling for investigating biophysical mechanisms.	• Lack of standardized measurement procedure leading to inconsistent results. • Need for larger sample sizes and longer-duration studies to validate the results. • Need for innovations in electrode technology and measurement devices to improve accuracy and signal quality. • Need to combine EIM with other sensing techniques for comprehensive assessments.
[10]	To review recent techniques in HAR, particularly on multimodal approaches, Deep Reinforcement Learning (DRL), and Large	• Reviews multimodal datasets encompassing heart rate, ECG, IMUs, PPG, EMG and thermal sensor for HAR. • Explores the use of LLMs in HAR, particularly for annotating large datasets and developing personalized HAR systems. • Reviews several DRL-based frameworks and their effectiveness in HAR tasks.	• Need for large datasets and efficient methods of labelling data is a challenge. • Improving the accuracy and reliability of HAR models, especially for complex activities remains a challenge.

Accepted Manuscript

	Language Models (LLMs).	• States the importance of multimodal fusion methods in HAR.	• lack of standardisation in data collection, communication protocols, and model representation affects HAR accuracy.
[27]	To explore and review the use of smartphone sensors, particularly accelerometers, for recognizing human gestures.	• Discusses the importance of gesture recognition in human-computer interaction (HCI), robot control, games, and surveillance. • Highlights different methods, including the use of digital pens and smartphone sensors for capturing and recognizing gestures. • Propose a cost-effective gesture recognition method using smartphone sensors.	• Lack of advanced algorithms and machine learning techniques to enhance recognition performance. • Need for efficient algorithms that can process and recognize gestures in real-time on smartphones. • Need to integrate accelerometer with other sensors to improve gesture recognition.
[28]	To provide a comprehensive review of energy-aware HAR techniques based on wearable sensors, excluding vision-based systems.	• Proposes a taxonomy of energy-aware strategies, categorizing them into sensor-based, system architecture and model design methods. • Analyses how different energy-aware techniques impact energy consumption and activity recognition accuracy. • Summarizes the state-of-the-art methods of reducing energy consumption.	• Need for developing and optimizing HAR algorithms for wearable devices. • Integrating multiple sensing modalities to improve accuracy while minimizing energy consumption. • Challenges of recognizing complex activities that involve high limbs or both high and low limbs.
[29]	To provide a comprehensive review of the current state and future directions in HAR using deep learning (DL) techniques.	• Analyses various sensor-based and video-based databases used in HAR, along with the performance metrics employed. • Compares major works that utilize DL models for various tasks in HAR. • Reviews advance in HAR applications, such as surveillance, healthcare and assisted living.	• lack of large-scale labelled datasets is a significant challenge. • Needs for a multi-sensory system, domain adaptation and hybrid techniques improve HAR performance. • High computational complexity of deep learning models is still a problem.
[30]	To provide a comprehensive overview of the current state of human activity recognition	• Proposes a taxonomy of HAR approaches into feature-based and learning-based approaches. • Provides detailed characteristics of HAR datasets such as number of videos and types of activities. • Compares HAR methods based on datasets and performance metrics.	• Many existing datasets lack diversity in terms of environmental conditions, occlusion, and multi-view scenarios. • Current HAR models struggle with generalization across different datasets and real-world scenarios.

Although significant progress has been made in the field of HAR, achieving accurate recognition of human activities and actions remains a persistent challenge. Notably, existing surveys have not explored the application of bioimpedance technology in this context. Bioimpedance measurement is a non-invasive, radiation-free, and cost-effective technique capable of detecting variations in body tissue impedance, providing real-time monitoring capabilities [18], [19], [31], [32], [33]. This review aims to investigate current technologies and methodologies that utilize bioimpedance measurement for physical activity monitoring, with a focus on recent advancements in activity recognition. The scope is confined to the applications of Electrical Impedance Myography (EIM) and Electrical Impedance Tomography (EIT), excluding Bioelectrical Impedance Analysis (BIA) for body composition, although its foundational principles are briefly acknowledged. Additionally, the review compares bioimpedance-based monitoring techniques with conventional methods in terms of accuracy, usability, and application scope. It further discusses the inherent limitations and challenges of

Accepted Manuscript

bioimpedance devices and outlines future directions for improving their reliability, precision, and practical utility.

The review offers the following significant contributions:

- It provides a discussion of the underlying principles of bioelectrical impedance analysis, electrical impedance myography, and electrical impedance tomography, establishing a foundational understanding of their respective mechanisms and applications.
- The review evaluates current electrode technologies used in bioimpedance sensing, with particular emphasis on innovations in textile-based dry electrodes that support wearable and long-term physiological monitoring.
- It demonstrates the practical utility of bioimpedance in real-time applications, including muscle activity monitoring, fatigue tracking, gesture recognition, neuromuscular disorders assessment, and respiratory and cardiac monitoring.
- The manuscript highlights the role of machine learning in enhancing bioimpedance signal interpretation and discusses the advantages of integrating bioimpedance with complementary sensing modalities.
- It identifies key limitations in bioimpedance-based activity monitoring and proposes future improvements through artificial intelligence integration, hybrid sensing systems, wearable technologies, and clinical validation.

1.1. Methodology of this Review

This review adopts a scoping review approach to systematically explore the current landscape of bioimpedance technologies applied to physical activity monitoring. The methodology follows the framework proposed by Arksey and O'Malley [34], in alignment with PRISMA-ScR reporting guidelines [35]. Relevant literature was identified through a structured search of peer-reviewed articles, technical reports, and review papers from complementary databases including PubMed, ScienceDirect, IOPscience, Frontiers and IEEE. Search terms were carefully selected to reflect the aim of the review and included bioimpedance analysis, human activity recognition, electrical impedance myography, electrical impedance tomography, muscle activity, gesture recognition, biopotential electrodes and wearable sensors.

1.1.1. Selection criteria

All included articles were peer-reviewed and published in reputable journals or conference proceedings and were written in English. Studies were eligible if they focused on bioimpedance-based sensing for activity recognition or physiological monitoring, presented experimental, theoretical, or review-based insights into Electrical Impedance Myography (EIM) or Electrical Impedance Tomography (EIT), and discussed the integration of bioimpedance with machine learning or wearable systems. Studies that focused solely on Bioelectrical Impedance Analysis (BIA) for body composition, without relevance to activity monitoring, were excluded.

Accepted Manuscript

A total of 924 related articles were initially identified across databases using the defined search terms. After removing duplicates and applying the screening criteria, 188 articles were selected for inclusion in the review. Figure 1 presents a schematic flow diagram outlining the study selection process.

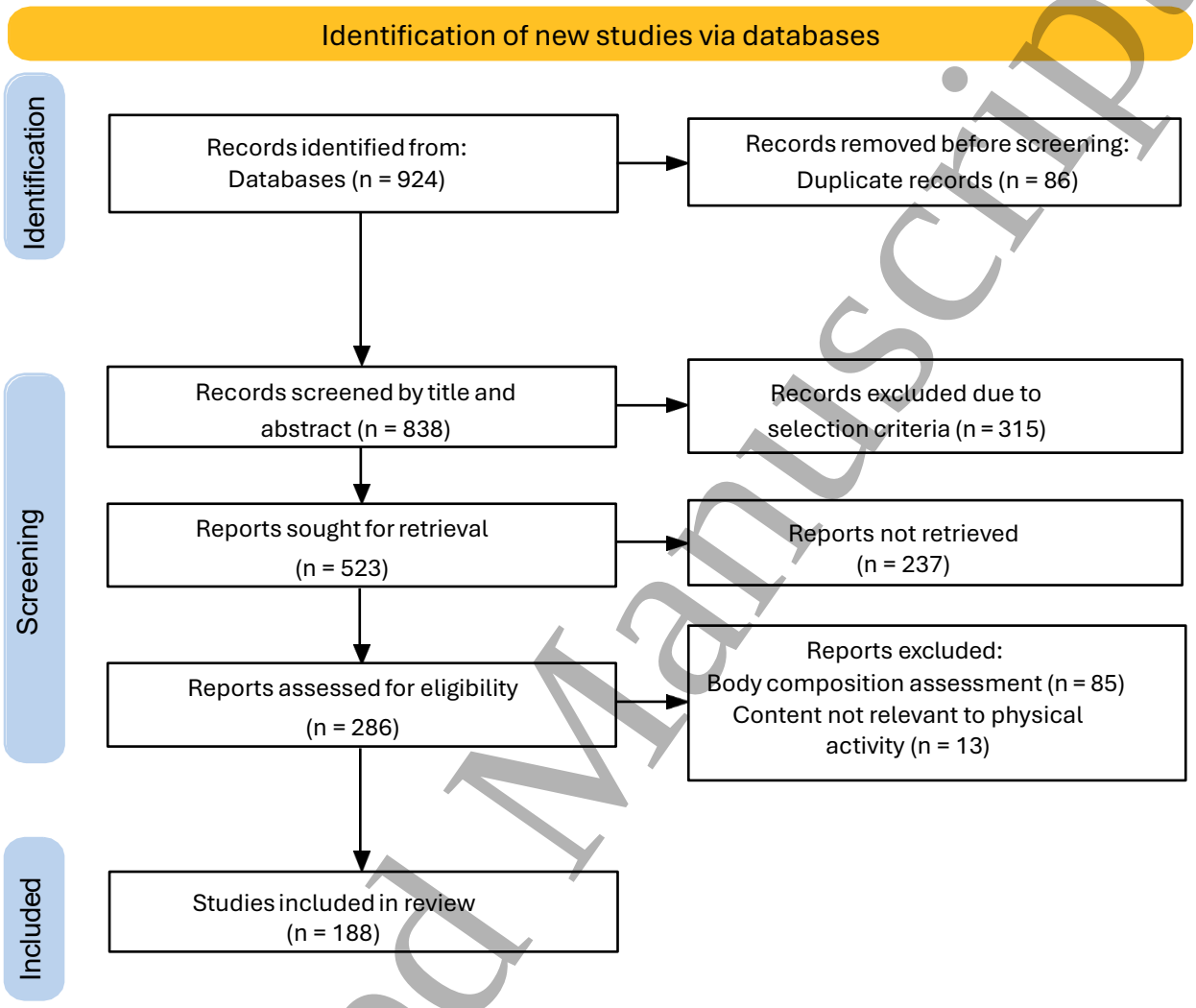

Fig.2: PRISMA flowchart of the study selection process

1.2. Bioimpedance technology

Bioimpedance technology applies a small alternating current, typically ranging from 100 µA to 10 mA, at frequencies between 1 kHz and 1 MHz to detect electrical impedance variations associated with physiological changes in biological tissues [36], [37]. The maximum safe current is prescribed in the standard IEC 60601-1. Research indicates that the electrical properties of body tissues vary with the frequency of the applied current [38]. The fundamental principle involves injecting high-frequency AC into biological material through electrodes and measuring the resulting voltage drop. This approach is based on Ohm's law, which states that the current flowing through a conductor is directly proportional to the potential difference across its ends, as expressed in Eq. (1).

$$V = IZ \tag{1}$$

Accepted Manuscript

where V = voltage (volts) and I = current (amps), Z = impedance (ohms). The impedance variation is computed as a function of frequency and is a complex number comprising a real part (electrical resistance, R) and an imaginary part (capacitive reactance, X_C) as shown in Eq. (2a) [39]. The phase angle (ϕ) of impedance indicates cell mass and membrane integrity, measured at the characteristic frequency. Higher values suggest better cellular function, while lower values are linked to disease, aging, or malnutrition [40].

$$Z(\omega) = R + jX_c \tag{2a}$$

$$\omega = 2\pi f \tag{2b}$$

$$|Z|(\omega) = \sqrt{R^2 + X_c^2} \tag{3}$$

$$\phi = tan^{-1}\left(\frac{X_c}{R}\right) \tag{4}$$

where Z = impedance, ω = angular frequency (rad/sec), R = electrical resistance, X_C = capacitive reactance, ϕ = phase angle, f = frequency and $j = (-1)^{1/2}$. The body tissue contains blood vessels and lymphatic channels acting as electrical conductors, with intracellular and extracellular fluids behaving like resistor-capacitor circuits [41]. However, the cell membrane functions as a capacitor, C_m, situated between conductive intracellular and extracellular fluids. It is connected in series with the intracellular fluid's resistance, R_i, and this series combination is then in parallel with the extracellular fluid's resistance, R_e, as illustrated in figure 2. The capacitive reactance, X_C is mathematically modelled using the formula

$$X_c = \frac{1}{\omega C_m} = \frac{1}{2\pi f C_m} \tag{5}$$

where X_C = capacitive reactance, f = frequency, $j = (-1)^{1/2}$, and C_m = capacitor. The relative permittivity (ratio of absolute permittivity, ε to vacuum permittivity, ε_o) of a material quantifies how the material responds to an applied electric field, influencing charge storage and polarization of the dielectric medium. It is influenced by water content and frequency of the applied electromagnetic field [41]. At low frequencies (e.g., <5 kHz), the high impedance of the cell membrane causes it to behave like an insulator, restricting current flow to the extracellular fluids. In contrast, at higher frequencies (e.g., >100 kHz), the impedance of the cell membrane decreases significantly, allowing current to pass through both extracellular and intracellular compartments. This frequency-dependent behaviour forms the basis of the Cole model, which describes how tissue impedance varies with frequency (see figure 3). In practice, frequencies such as 5 kHz and 100 kHz are commonly employed as empirical proxies for the theoretical limits of 0 Hz and ∞ Hz, respectively, to estimate extracellular and total body water content. Therefore, bioimpedance variations are influenced by the physiological and pathological changes in the tissue composition [39].

Accepted Manuscript

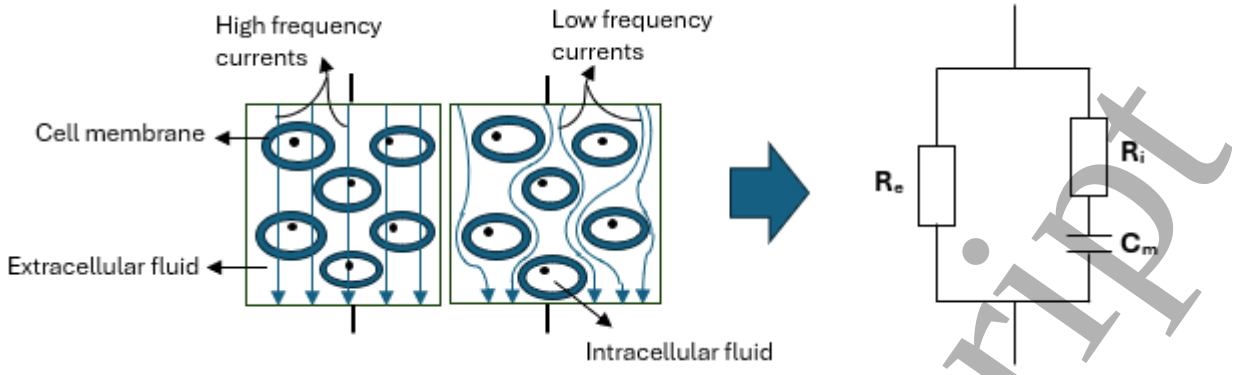

Fig.3: Cell structure and electrical equivalent circuit for biological tissues

Figure 3 depicts the Cole model for biological tissues [40]. It represents the extracellular pathway of electric current by a single resistor (R_e) in parallel with the resistance of intracellular fluid (R_i) and a capacitor (C_m) indicating the surrounding cell membranes. Thus, the impedance (Z) of this equivalent circuit (Cole model) at a specific angular frequency (ω) is given by [42].

$$Z = R_\infty + \frac{R_o - R_\infty}{1+(j\omega\tau)^\alpha} \quad (6)$$

where R_∞ is the resistance at infinite (high) frequencies, R_o is the resistance at zero (low) frequencies, $j = (-1)^{1/2}$, τ is the characteristic time constant for a capacitive circuit and α is the coefficient of relaxation in the Cole equation and depends on the property of the tissue layer. It ranges between 0, indicating perfectly homogenous tissue and 1, indicating perfectly heterogeneous tissue ($0 < \alpha < 1$) [43]. Accordingly, Eq. (6) becomes the Fricke–Morse model when the value of $\alpha = 1$ [44]. In the α–dispersion frequency range (1kHz – 100kHz), current associated with reactive impedance predominantly flows in the extracellular fluid due to movement of ions. It has been reported that the relative capacitance shows a tendency to decrease in this frequency range [26]. In β-dispersion frequency range (100kHz – 10MHz), the ion movement interaction increases, and the capacitance effect of the cell membrane decreases, thus, allowing more current to pass through the cell membrane easily [26].

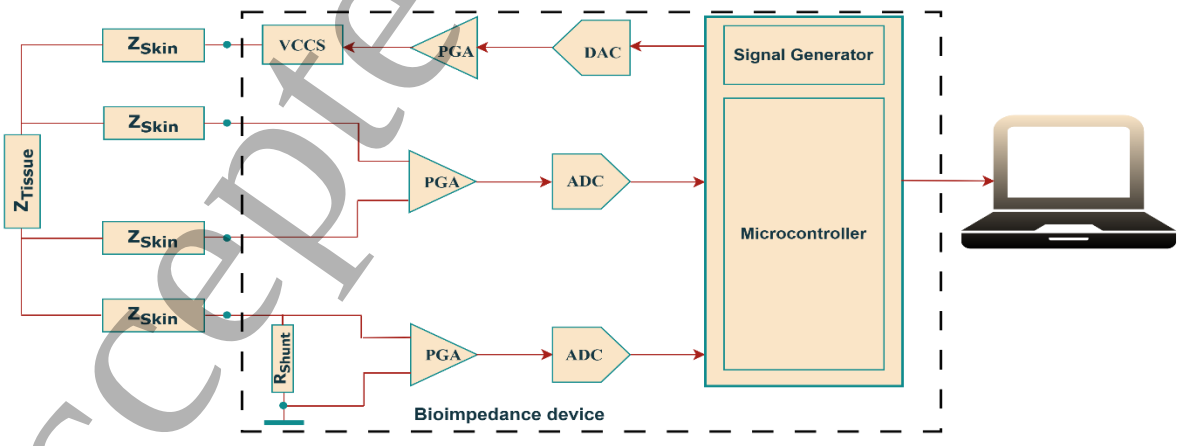

Fig.4: Block diagram of bioimpedance measurement system. where VCCS = Voltage controlled current source, PGA = Programmable gain amplifier, DAC = Digital to analogue converter, ADC = Analog to digital converter, R_{Shunt} = Shunt-resistor, Z_{Tissue} = Tissue impedance, Z_{Skin} = Contact impedance between skin and electrode.

Accepted Manuscript

The bioimpedance measurement system consist of a signal generator for current injection at variable frequency, electrodes for driving current and measuring voltage drop and a microcontroller as shown in figure 4. The electrode arrangement depends on their number and placement, with two common configurations: two-electrode and four-electrode terminal schemes.

The two-electrode (bipolar) terminal scheme uses the same electrodes for current injection and voltage measurement, resulting in a low-cost, compact and simple circuit design as shown in figure 5a. However, contact impedance at the electrode-skin interface causes inaccuracies, and signal quality is compromised due to interference [45]. Despite these limitations, it is still sometimes used for impedance measurement [46], [47], [48].

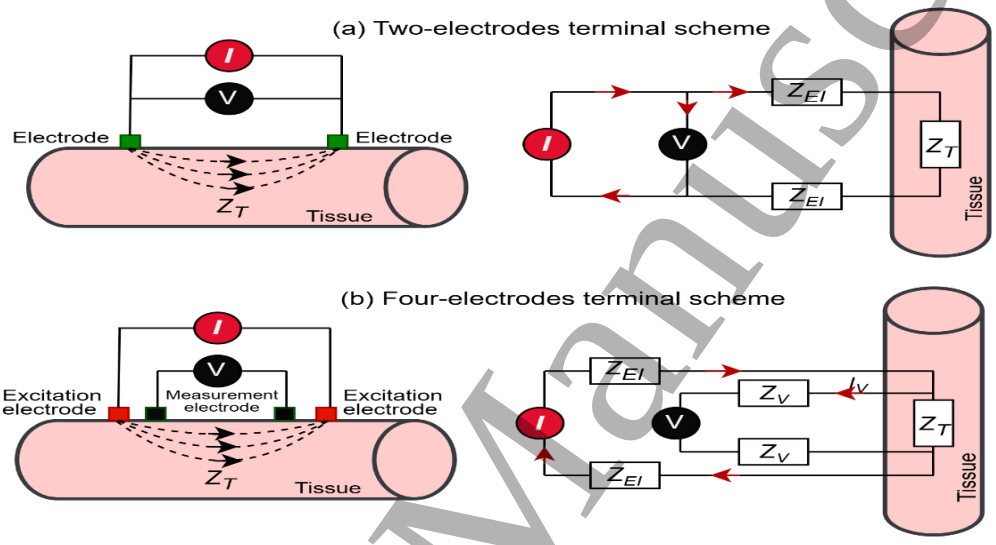

Fig.5: Electrode terminal scheme and electrical equivalent circuits. where I = Excitation current, V = Voltage, Z_T = Tissue impedance, Z_{EI} = Excitation current impedance, Z_V = Voltage impedance.

The four-electrode (tetrapolar) terminal scheme uses separate pairs of electrodes for current injection and voltage measurement, ensuring measurements are independent of electrode-skin contact impedance as shown in figure 5b. Although this configuration is more costly and complex, it provides uniform current distribution, no electrode polarization, [26] allowing for accurate real-time monitoring of for instance, hemodynamic parameters like the pulsatile ulnar artery [31], stroke volume and cardiac output [19]. Tetrapolar electrode configurations are widely used in bioimpedance systems for their high measurement accuracy. However, they present practical challenges such as electrode mismatch [49], aging [50], placement sensitivity [51] and phase error due to parasitic capacitance [52], which can affect signal quality and consistency. Addressing these factors is essential to ensure reliable and reproducible results. Studies have shown that physical factors such as intrinsic impedance and electrode material (e.g., Ag/AgCl) can cause measurable shifts in bioimpedance vectors, which may result in misinterpretation of physiological parameters if these factors are not adequately considered [53]. Therefore, standardized performance testing and careful electrode selection are essential to ensure consistency in tetrapolar bioimpedance systems [54].

1.3. Biopotential Electrode Materials

Accepted Manuscript

Biopotential electrodes are essential for accurate bioimpedance measurement, being non-invasive and conductive. The signal quality detected strongly depends on electrode-skin impedance, which varies between individuals [55]. However, high electrode contact impedance reduces signal quality, amplitude, and signal-to-noise ratio, but can be improved by increasing the pressure and contact area between the electrode and skin as well as applying conductive fluid on the skin in contact with the electrode [56].

Biopotential electrodes are either polarizable or non-polarizable [55]. Polarizable electrodes, like stainless steel, have high impedance at low frequencies, and do not allow significant charge transfer across the electrode-skin interface. However, they can be reused due to their resistance to corrosion [57]. Non-polarizable electrodes, such as silver/silver chloride (Ag/AgCl), have low impedance and allow charge transfer due to an electrolyte gel [55]. However, the gel can cause skin irritation or itchiness over long recordings, and they become less effective as they dry out [58]. Ag/AgCl electrodes are preferred in clinical and research settings for their low impedance and high signal quality [55].

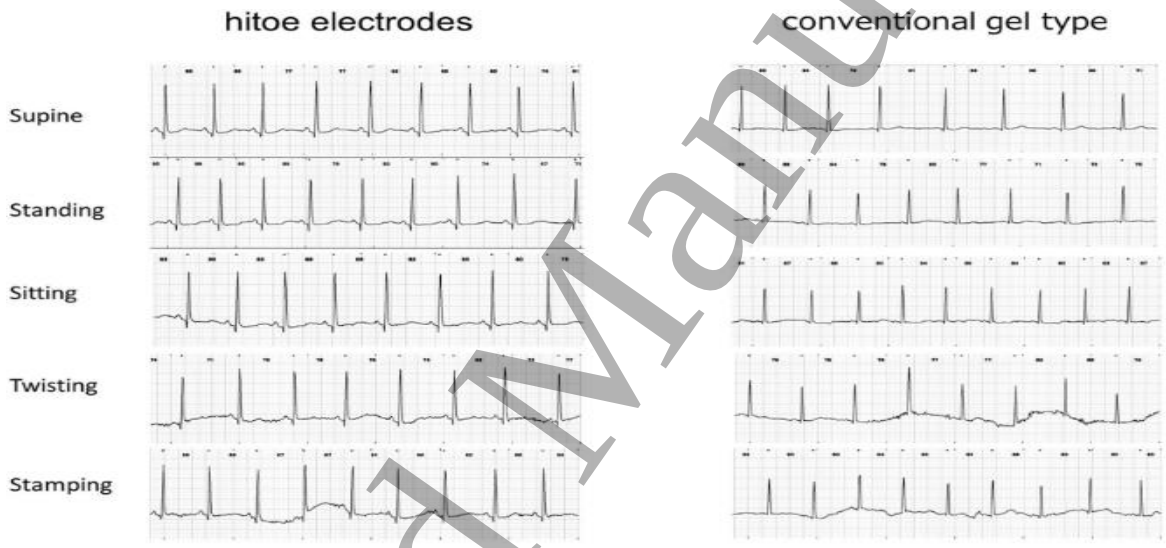

Fig.6: Biopotential signals for textile (hitoe) and conventional gel electrodes. Reproduced from Tsukada et al. [63]

In recent years, textile dry electrodes have become popular for biopotential measurements due to their integration into wearable materials, enabling long-term monitoring [59], [60]. Hu et al. [61] proposed textile electrodes integrated with a clothing belt to reduce discomfort and improve electrode-skin contact while Rutkove et al. [62] demonstrated that electrode position and size significantly affect bioimpedance measurements. Studies show electrocardiogram (ECG) patterns (P, QRS, and T waves) recorded with textile electrodes are comparable to conventional gel electrodes [63] (see figure 6). However, hybrid textile electrodes can monitor and capture ECG signals and physical activities in real time with minimal noise [64]. Adaptive filtering method helps to reduce motion artifacts in wearable ECG monitoring systems [65], [66], [67]. Table 2 depicts current studies on electrophysiological sensing using textile electrodes.

Accepted Manuscript

Table 2: Summary of Some Previous Studies on Electrophysiological Sensing using Textile Electrodes.

Author	Electrode Material	Aim	Advantages	Limitations	Results
Tsukada et al. [63]	Hitoe (Nano-fibre yarn coated with PEDOT-PSS)	To develops textile electrode and compare with traditional gel electrode for performance	• Wearable for ECG monitoring in daily life. • No skin irritation after long use.	Sensitive to motion artifacts during vigorous movements	• Good signal quality with lower Signal-to-noise ratio. • Suitable for long-term and repeated use
Nigusse et al. [59]	Silver-printed polyester	To provide a good alternative to Ag/AgCl used in long-term ECG monitoring	• Suitable for long-term ECG monitoring • No skin penetration	Reduces signal quality slightly during vigorous movements	• Good signal quality but embroidered electrode shows better quality. • Retained performance after washing.
	embroidered conductive				
	silver-plated conductive hook				
Monti et al. [68]	Textile Elastic band with Shielded Technik-tex P180 + B by Statex	To provide a comfortable, wearable solution for continuous monitoring.	• Suitable for continuous monitoring. • Easily integrated into wearable systems.	Focused on a specific age group and ethnicity.	• No significant difference in signal quality with gel electrode • Consistent repeatable results.
Cho et al. [69]	Cu-Sputtering fabrics	To develop and evaluate textile-based electrodes and motion sensors for smart clothing.	• Applicable in health monitoring. • Efficient in monitoring athletic performance and in rehabilitation exercises.	Low signal quality during dynamic conditions	Good flexibility and conductivity, with average of 1.27 Ω (PU laminated)
	Cu/Ni Electroless Plating				Lower resistance (0.23 Ω) compared to the Mesh fabric (0.29 Ω).
	Embroidered stainless Steel Filament Yarn				Best performance in terms of peak detection rates.
Wang et al. [70]	SMP130-B	To identify suitable textile materials for long-term bioimpedance monitoring	• More comfortable than Ag/AgCl electrodes. • Better current distribution than spot electrodes.	Textiles SBRM48 performed poorly due to poor contact with the skin.	• SMP130T-B had the highest precision but expensive. • Textile electrodes provided more uniform current distribution.
	Stretch				
	SMP130T-B				
	SBRM48				
	SBAL317				
Martins et al. [71]	Elitex SC fibres	To integrates sEMG and IMU into e-textile smart vest for monitoring forward head posture.	• Suitable for both dynamic and static conditions. • System's accuracy is sufficient for typical cervical movements.	Not Stated	• Elitex SC fibres performed better than Shieldex fibres. • 4 × 2 cm textile electrodes performed similarly to Ag/AgCl electrodes.
	Shieldex fibres				
Marquez et al. [72]	Synthetic wrap knitted with silver fibre	To evaluate the performance of textile-based dry	• Suitable for BIS measurements.	Bad reliability for body	• Textile electrodes exhibited lower resistance values (R_0

Accepted Manuscript

	adhesive conductive gel	electrodes and compare with standard gel electrodes.	• large contact area of textile electrodes helps mitigate polarization impedance	composition analysis.	and R_∞) and higher characteristic frequency compared to gel electrodes.
Li et al. [73]	Deep reactive ion etching (DRIE) and isotropic wet etching. Microneedles coated with a Ti/Au layer.	To develop and evaluate a novel microneedle electrode array (MEA) for EIM to assess neurogenic myopathy.	• Contact area does not affect MEA contact impedance. • Suitable for long-term monitoring, and reusability.	Refinement is needed to optimize the design and enhance clinical applicability.	• MEA exhibited lower contact impedance compared to wet electrodes especially at low frequencies. • MEA gave excellent test-retest reproducibility with ICC of 0.92
Arquilla et al. [74]	Sewn with silver-coated thread	To explore the feasibility of using sewn textile electrodes for ECG monitoring in wearable health systems.	• Suitable for long-term health monitoring. • Good durability under stretch, bend, and wash conditions.	Not stated	• No significant difference between traditional and textile electrodes for R-R interval and heart rate. • no significant change in resistance after bend and stretch.
An et al. [75]	Silver-plated knitted conductive fabric	To investigate the performance of textile electrodes for wearable ECG monitoring	• Suitable for long-term wearable applications and can be integrated into garments for constant health monitoring	Highly sensitive to position changes compared to wet electrodes.	• Larger electrodes and increasing holding pressure reduces skin-electrode impedance. • Optimal pressure of 30mmHg (4 kPa) was identified as comfort.
Meghrazi et al. [76]	Silver-plated and Carbon-coated nylon yarns knitted into fabric	To develop and evaluate textile-based multichannel ECG band to measure ECG signals from waist locations.	• The History-Dependent Inverse Gaussian (HDIG) algorithm enhances R-peak detection accuracy.	ECG signal quality is influenced by body position and motion artifacts.	• Shape of QRS wave form comparable to gel electrodes. • Higher accuracy and F1-score for R-peak detection

2. Forms of Bioimpedance Measurement

The accuracy of bioimpedance measurement depends on the method used, which varies based on frequency, measurement technique, and compartment model. The primary types of bioimpedance measurement applied in research studies, clinical and health monitoring are commonly known as:

- Bioelectrical impedance analysis: Predominantly applied for the assessment of body composition.
- Electrical impedance myography: Primarily used to evaluate muscle health and function.
- Electrical impedance tomography: Commonly employed for imaging purposes, offering spatially resolved insights into internal physiological structures.

Accepted Manuscript

Although these modalities are all based on bioimpedance principles, they differ significantly in electrode configuration, excitation strategy, and clinical applicability. Table 3 provides a comparative summary of key parameters across the three techniques.

Table 3: Comparison of typical BIA, EIM and EIT systems

Modality	Electrode Type	Number of Electrode	Electrode Placement	Excitation Frequency / Spectrum	Application	Sample Size & Subject Type
Bioelectrical impedance analysis (BIA)	Ag/AgCl, textile electrodes	2 - 4	Hand-foot or segmental	Single-frequency (e.g., 50 kHz), multi-frequency, or spectroscopy (1 kHz-1 MHz)	Body composition assessment (fat mass, water content, muscle mass)	Often healthy adults; used in clinical, fitness, and elderly populations
Electrical impedance myography (EIM)	Ag/AgCl, microneedle, and textile electrodes	2 - 4	Over specific muscles (e.g., biceps, thigh)	Single, scanned and multi-frequency (1 kHz-1 MHz)	Muscle health monitoring, fatigue detection, neuromuscular disorder assessment	Small clinical cohorts, athletes, patients with ALS, SCI, or stroke
Electrical impedance tomography (EIT)	Textile, copper, and gel electrodes	8 - 64	Circular arrays around limbs or torso	Single, dual, or multi-frequency	Gesture recognition, respiratory monitoring, and rehabilitation assessment	Healthy subjects and clinical patients; sample sizes vary across studies

2.1. Bioelectrical Impedance Analysis

Bioelectrical Impedance Analysis (BIA) is a widely used method for assessing body composition, including body fat percentage, muscle mass, and total body water [77]. It provides useful biological understandings about the physical and electrochemical processes in the body tissues and hence, are effective for monitoring various physiological variations [19]. Measures of bioelectrical conductivity are proportional to total body water, free-fat and skeletal muscle mass. The measurement is based on the relationship between the volume of the conductor (body), the conductor's length (height), and its electrical impedance as shown in Eq. (7).

$$Volume = \frac{\rho L^2}{Z} \tag{7}$$

where ρ is the resistivity of the blood, L = length of conductor and Z = impedance. Nevertheless, the human body is not a homogeneous cylinder, and body composition estimation from impedance requires several assumptions, including constant body geometry and composition of the fat-free body. Traditionally, this estimation has relied on empirical correlations and multiple regression analysis [78]. However, for a more physiologically grounded analysis, mixture theory modelling such as the Cole model is employed to account for the heterogeneous and frequency-dependent electrical properties of biological tissues [40].The accuracy and reliability of BIA depend on the underlying compartment model, which represents the body as distinct components that influence electrical conduction.

Accepted Manuscript

Various compartment models are used to improve the precision of body composition assessment [79]. For example, a two-compartment (2C) model divides body weight into fat mass (FM) and fat-free mass (FFM) and is widely used in clinical and fitness settings [33]. More advanced models, such as the three-compartment (3C) model which includes FM, total body water (TBW), and dry fat-free mass (dFFM), and the four-compartment (4C) model which further separates TBW into intracellular water (ICW) and extracellular water (ECW) provide more detailed assessments, particularly for athletes, clinical patients, and elderly individuals [33], [79]. However, it is important to note that BIA, including its spectral variants, is fundamentally based on a 2C model.

The impedance of the body tissue can be obtained using single-frequency, multi-frequency or bioelectrical impedance spectroscopy. Single-frequency bioelectrical impedance analysis (SF-BIA) applies a small alternating current (typically at 50 kHz) through the body and measures the resulting impedance [80], [81] (see figure 7a). It estimates total body water (TBW) but cannot directly differentiate intracellular (ICW) from extracellular water (ECW) [78]. However, empirical models based on population data allow approximate ECW and ICW estimation by assuming a stable ECW/TBW ratio in healthy individuals [82], [83]. Many commercial SF-BIA devices apply these models, though accuracy decreases in populations with altered fluid distribution [84]. In contrast, multi-frequency bioelectrical impedance analysis (MF-BIA) applies electrical currents across a range of frequencies to distinguish between ECW and ICW compartments more accurately [33], [83], [85] as shown in figure 7b. This approach enhances accuracy and assesses hydration status, muscle mass, and overall health more precisely [86].

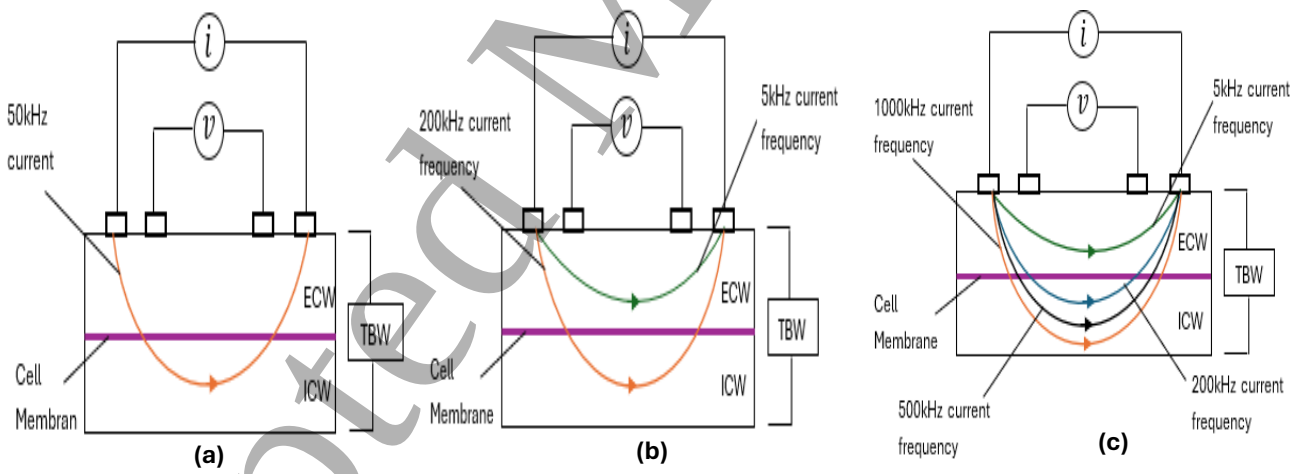

Fig.7: (a) Single-frequency BIA method, (b) multi-frequency BIA method, (c) bioelectrical impedance spectroscopy method, where i = excitation current, v = voltage

Bioelectrical impedance spectroscopy (BIS) measures body composition and fluid distribution over a range of frequencies, f (f_1, f_2, f_3, ..., f_n) typically from 1 kHz to 1MHz as shown in figure 7c [19], [87], [88]. BIS uses mathematical modelling (Cole analysis and Hanai mixture theory) to estimate body water distribution and cell membrane integrity, making it more advanced than MF-BIA [33], [89]. Recent studies has applied BIS in estimating blood flow-induced physiological variations [19], [90], characterizing muscle tissue [91], [92], diagnosing malnutrition in chronic kidney disease patients [93], [94], determining fruit maturity in real

Accepted Manuscript

time [95], analysing and characterising different biological materials [96], [97]. Khalil et al. [98] have discussed methodically the fundamentals, measurement techniques, influencing factors, and clinical applications of BIA in clinical monitoring and disease diagnosis.

2.2. Electrical Impedance Myography

Electrical Impedance Myography (EIM) is a non-invasive, painless technique used to assess muscle health by injecting a weak, high-frequency electrical current, typically between 100 µA to 1 mA, to muscle tissue, and measuring the resulting surface voltage drops [99]. However, it mostly depends on the changes in the electrical properties of the tissue layers of the muscle and internal body structure in response to applied current signals at different measurement frequencies and directions [26] (see figure 8).

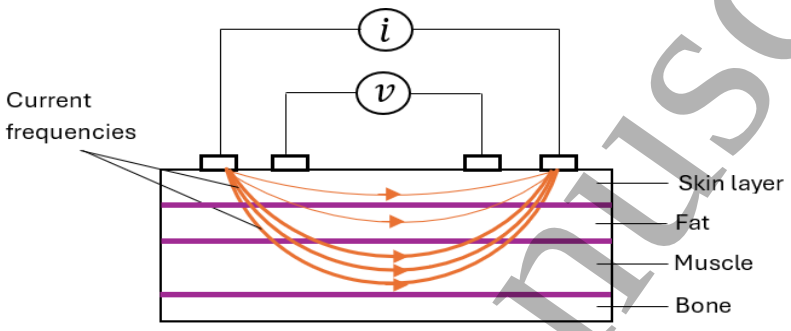

Fig.8: Schematic diagram of EIM measurement technique

The EIM assesses the impedance changes in biological tissues which indicate abnormal muscle conditions, such as muscle fibre loss, atrophy, edema and fatty infiltration, and could serve as a valuable tool for quantifying the severity of diseases that affect the muscles [100]. The impedance values computed reflect the inherent properties of the muscle, including resistance (R), capacitive reactance (X_C), phase angle (ϕ), and anisotropy ratio (AR). However, the phase angle calculated based on R and X_C values evaluates the membrane oscillation properties of the muscle whereas, AR values, affected by electrode size, spacing, and orientation relative to the muscle fibre signify the degree of columnar order in the arrangement of the fibres [101].

Muscle anisotropy refers to how the impedance values vary depending on the orientation of the applied current relative to the muscle fibre direction. Muscle fibres are organized in a parallel structure, leading to different impedance values when current flows along (longitudinal) or across (transverse) the fibres. Higher conductivity is exhibited when current flows along the muscle fibres and lower, when it flows across the fibres [26]. The ratio of muscle impedance in transverse direction, Z_{Trans} to muscle impedance in longitudinal directions, Z_{Long} is called the anisotropy ratio, AR of the muscle [102] and can be computed using Eq. 8.

$$AR = \frac{Z_{Trans}}{Z_{Long}} \tag{8}$$

A higher anisotropy ratio indicates a healthy muscle whereas lower anisotropy ratio indicates a diseased muscle. EIM has an advantage of being painless and using low intensity current (<1 mA) over the conventional neuro-electrophysiological methods, such as needle electromyography (EMG). This helps to avoid neuromuscular excitement [73]. The method of

Accepted Manuscript

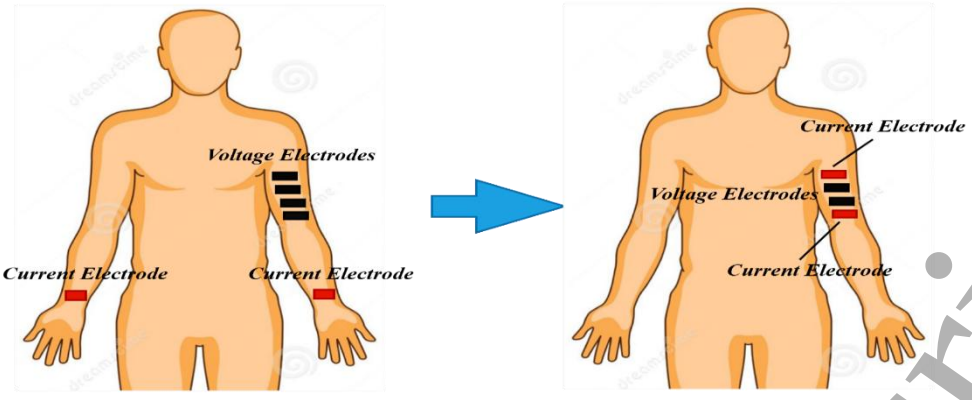

Fig. 9: Evolution of EIM measurement technique from far-current electrode (left) to near-current electrode (right).

EIM assessment reported in literature has evolved from the far-current electrode technique to linear-EIM or near-current electrode technique as shown in figure 9 [62]. When using a far current electrode technique, the voltage of the muscle of interest is the average of the measured voltages across each pair [103]. A numerical investigation on optimizing electrode configuration for EIM shows that adjustments in the electrode arrangement can significantly impact the impedance data and its sensitivity to morphological variation [104].

Presently, linear-EIM is mostly executed using a four-electrode terminal configuration and the measurement results depend on current and voltage electrode positions. To optimize measurement accuracy, many studies have used microneedle electrode arrays [73], finite element models based on various equations [104], [105] and moved the electrodes to different places throughout the muscle of interest until a better location was found [62], [106]. Moreover, studies have shown that the muscle is anisotropic, and impedance varies based on electrode orientation relative to muscle fibres [107]. A comprehensive assessment of the impedance characteristics of the muscle in different orientations can be achieved by varying the direction of the applied current flow via rotating the current and voltage electrodes around a central point over the muscle of interest (see figure 10) [107].

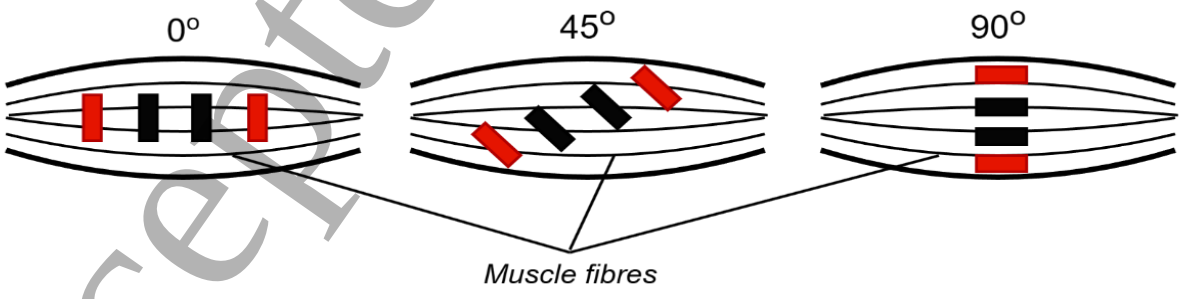

Fig. 10: The basic concept of rotational EIM.

2.2.1. Frequency-Dependent measurements in Electrical Impedance Myography

Accepted Manuscript

In EIM assessment, the electrical properties of the muscle vary with frequency and direction [108]. However, the impedance change of the muscle can be obtained through single, scanned or multi-frequency measurement analysis.

2.2.1.1. Single-Frequency EIM

Single-frequency measurement is commonly used for basic clinical assessment. It has been reported that the biological tissue tends to be most sensitive at or near a frequency of 50 kHz [107]. Hence, most commercially available cost effective EIM devices emit electrical current at a fixed frequency of 50 kHz. Although single-frequency measurement provides limited information about the muscle of interest, it can be used in evaluating the health of specific muscles such as abductor pollicis brevis [107].

2.2.1.2. Scanned-Frequency EIM

This measurement technique involves sending out excitation current with different frequencies at intervals over some time to obtain muscle impedance information at multiple discrete frequencies [26] as shown in figure 11. It provides more information in the frequency domain, but does not capture continuous or fast changing dynamic processes [109]. Both single and scanned frequency EIM measuring devices have limitations in applications requiring real-time monitoring. Most commercially available broadband bioimpedance devices, such as the Keysight E4990a operating within a frequency range of 20 Hz to 120 MHz [110], ImpediMed SFB7 operating within 3 kHz to 1000 kHz [111], and the Zurich Instruments MFIA operating within 1 mHz to 5 MHz employ scanned-frequency methods to measure impedance across a wide frequency spectrum.

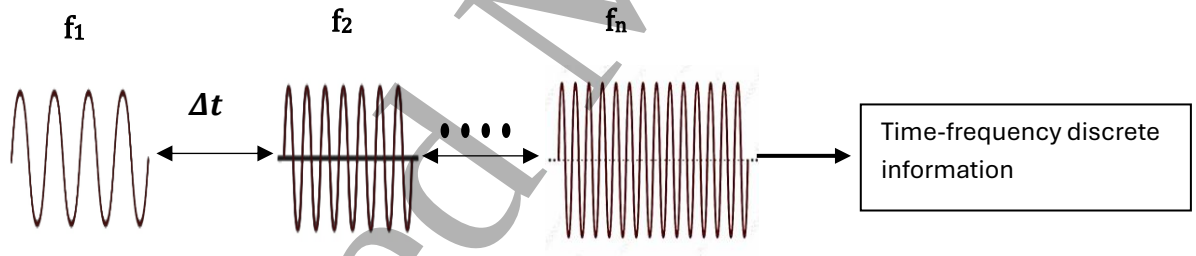

Fig. 11: Scanned-frequency signal excitation

2.2.1.3. Multi-frequency EIM

This has emerged as a conventional muscle impedance measurement method due to its ability to capture time-varying information in dynamic processes [112]. However, it entails injecting excitation currents with different frequencies ranging from 1 kHz to 1 MHz simultaneously within a signal cycle, to obtain impedance continuous time-frequency data after processing the mixed signals using the Discrete Fourier Transform (DFT) [113] (see figure 12). The measurement time at any period is determined by the signal with the lowest frequency. Subsequently, recent studies have shown that electrical impedance across a spectrum of applied frequencies and with current flow at multiple orientations relative to the direction of muscle fibre can provide a more comprehensive insight into muscle structure and health [108], [114].

Accepted Manuscript

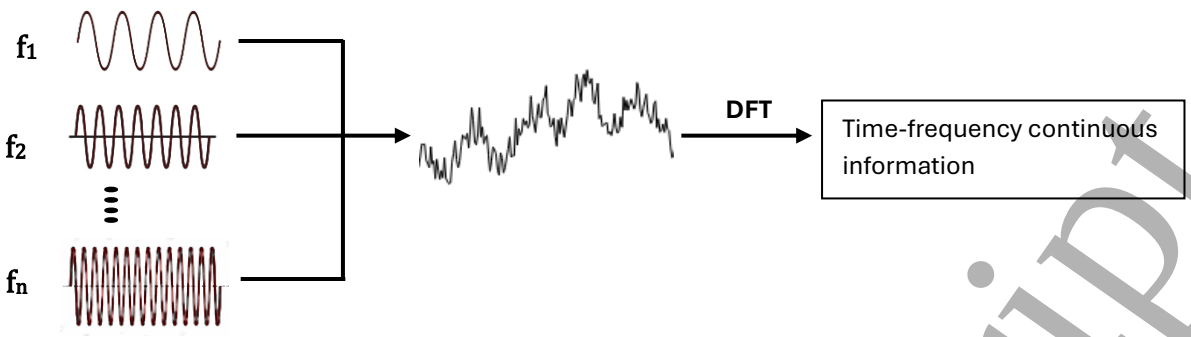

Fig. 12: Multi-frequency signal excitation

2.3. Electrical Impedance Tomography

Electrical Impedance Tomography (EIT) is a painless, non-invasive, radiation-free imaging modality that has gained attention in various fields, including human machine interaction, medical diagnostics, industrial monitoring, and, more recently, activity recognition [115]. It is a process of reconstructing and displaying images of the electric conductivity and permittivity of tissue inside the body [116]. The EIT measurement system detects the internal changes in the conductivity of the body's tissue caused by human activities [56]. These internal changes arise from variations in muscle deformation, posture, blood flow, and lung expansion, which alter the electrical impedance [117]. This electrical impedance refers to, when a small current is introduced through electrodes placed on the surface of the body, the resulting voltage measurements are used to reconstruct an image of the internal impedance distribution [115], [118] as shown in figure 13.

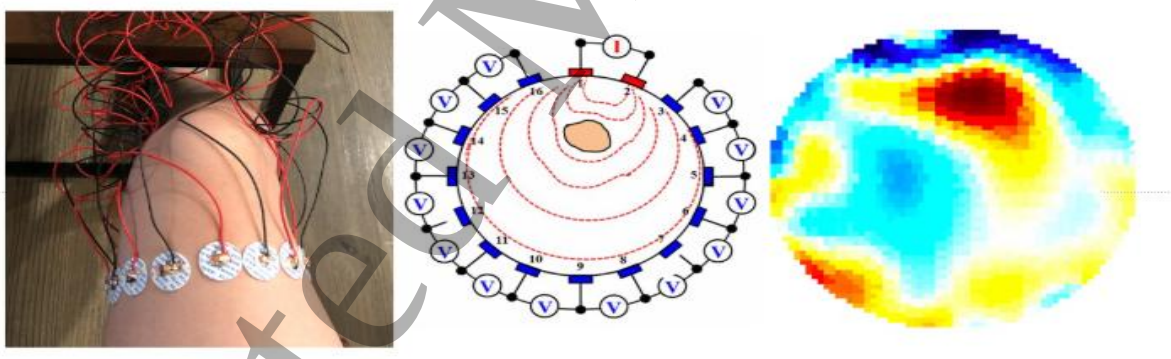

Fig. 13: EIT measurement technique. Reproduced from Zhu et al. [115]

Additionally, EIT provides a unique capability to monitor and compute both absolute and differential imaging in real-time using wearable devices. Absolute imaging refers to impedance values that represent the distribution of conductivity at a specific time without using reference data. However, it is more computationally intensive and susceptible to noise, resulting in lower image resolution. In contrast, differential imaging refers to impedance values that represent the conductivity distribution between two time points, is less affected by noise and relatively easier to calculate [37]. The differential imaging can either be time-difference or frequency-difference imaging [39]. Time-difference imaging refers to difference of impedance at different times on the same excitation frequency. It requires a baseline impedance measurement to compare

Accepted Manuscript

subsequent measurements in order to detect variations caused by physiological changes. It is also highly sensitive to dynamic changes, less sensitive to electrode positioning errors and suitable for real-time monitoring [119]. Frequency-difference imaging refers to the difference of impedance at different frequencies at the same time. It provides information about tissue properties and structure and does not rely on baseline impedance measurement to recognise variations. Nevertheless, it is highly sensitive to instrumentation errors, has lower temporal resolution and is less sensitive to motion.

The excitation frequency used in EIT measurements can either be conventional, dual frequency or multi-frequency [120]. Conventional EIT applies single frequency (typically 50kHz) detects changes in conductivity by constructing images from two measurements at two different times, whereas dual frequency EIT detects changes in conductivity as a function of frequency. It injects currents at two different frequencies simultaneously, allowing voltage to be measured between two types of layers, thus revealing differences in their cellular structure. However, in multi-frequency EIT, the specific conductivity of each tissue varies with frequency, and currents are injected at different frequencies, either sequentially or simultaneously [120].

2.3.1. Methodological Considerations in EIT measurements

The accuracy and quality of EIT images primarily depend on electrode placement, injection/measurement method and image reconstruction technique [121], [122]. Optimizing these factors improves spatial resolution, reduces artifacts, and enhances the reliability of reconstructions.

2.3.1.1. Electrode Placement Schemes

The placement and number of electrodes significantly influence the image resolution and accuracy of EIT-based activity recognition [122]. However, electrodes in circular arrays are commonly used when monitoring symmetrical body regions as presented in this study [119], while customized arrangements have been explored for irregular surfaces. Electrode placement can be classified into 2D (planar) and 3D (volumetric) configurations [123]. The 2D configuration refers to the placement of single electrode array on a circular surface, forming a single cross-sectional plane of measurements. Additionally, it is cost effective, simpler and suitable for real-time monitoring applications. The 3D electrode configuration refers to the placement of double electrode arrays on a circular surface, forming a double horizontal layer cross-sectional plane of measurements [124], [125] as show in figure 14.

Accepted Manuscript

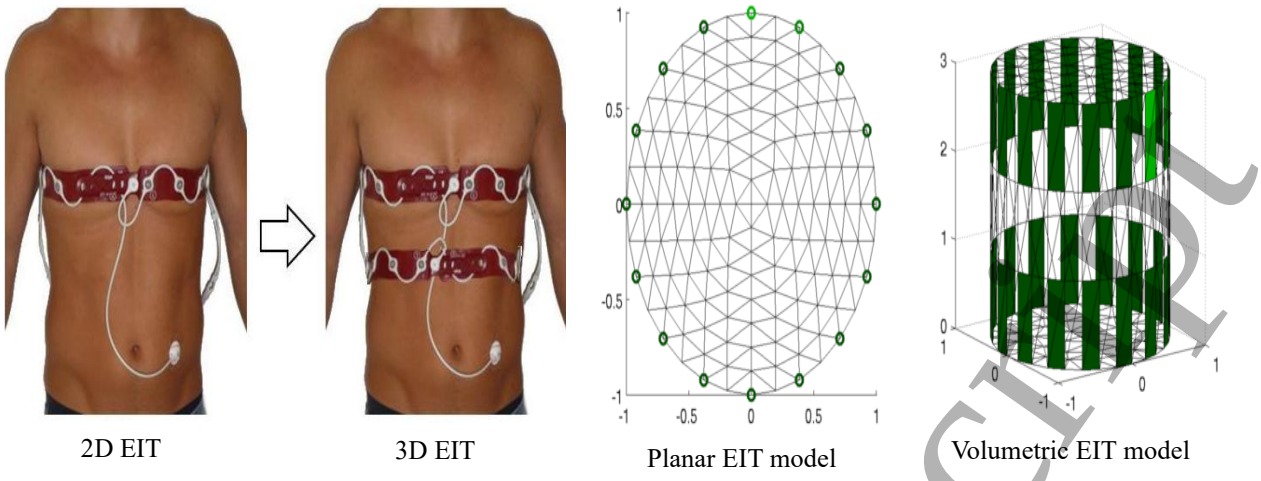

Fig. 14: EIT electrode configuration. Reproduced from Schullcke et al. [125], and Adler [133]

The 3D configuration improves sensitivity to deep structures, captures volumetric imaging and provides a more complete representation of conductivity distribution within the body tissue [123]. However, the image resolution performance in 3D EIT depends on the spacing between the upper and lower electrode planes of the two-plane EIT sensor [124]. The investigation on the effect of using multilayer electrodes has proven that 3D EIT performs better than 2D EIT in gesture recognition [123], [125]. The number of electrodes commonly used in EIT systems are eight (8), sixteen (16), thirty-two (32), or sixty-four (64) [117]. Recent studies has shown that increasing electrode count strictly improves spatial resolution and recognition accuracy but reduces temporal resolution and increases computational complexity and hardware requirements [45], [120].

Problems arising from positioning of the electrodes on the boundaries for image reconstruction algorithms has been a major concern, especially for medical applications, in which the body surface moves during breathing and posture change. However, Soleimani et al. [126] develop a method which directly reconstructs both electrode movements and internal conductivity changes for 2D and 3D EIT, and Pennati et al. [39] suggests using an elastic or adjustable electrode belt in wearable EIT systems for different body sizes. Also, Wang et al. [122] address the limitations of traditional EIT systems, particularly the fixed number of electrodes and their placement constraints, which restrict flexibility and adaptability in wearable healthcare imaging applications.

2.3.1.2. EIT Excitation and Measurement Mode

The excitation and measurement mode in EIT describes the process by which an alternating current, typically ranging from 100 µA to 10 mA and spanning frequencies from 0.1 Hz to 100 kHz [37], [127], is injected into body tissue via electrodes, while the resulting voltage drops are measured [36]. However, the quality of the reconstructed image, internal impedance distribution and reconstruction accuracy depend significantly on the type of measurement configuration employed [121]. EIT excitation and measurement techniques are typically in adjacent, cross or opposite drive patterns as shown in figure 15 [127].

Accepted Manuscript

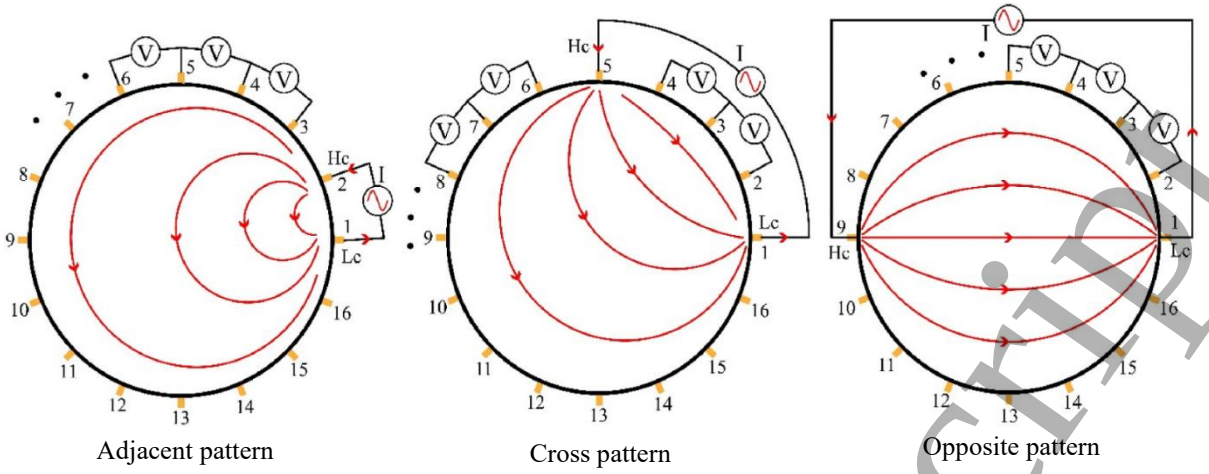

Fig. 15: EIT current excitation and measurement configuration. Reproduced from Li et al. [127].

In adjacent (neighbouring) measurement patterns, the current is applied between two neighbouring electrodes and voltage drops are measured between the next adjacent electrode pairs. Consequently, for n-electrodes using a four-electrode terminal scheme, there will be $(n-3)$ voltage recordings for each current injection and thus, a total of $n(n-3)$ voltage recordings [121] while there are total of $n(n-1)/2$ voltage recordings in a two-electrode terminal scheme. Although this configuration has poor penetration depth, it is simple and widely used in medical applications due to its high sensitivity near the boundary [127]. On the other hand, a cross (diagonal) measurement pattern improves sensitivity in central regions but is complex and computationally intensive while, the opposite (polar) measurement pattern enhances penetration and improves sensitivity in the centre, making reconstruction less accurate at the boundary.

2.3.1.3. Image Reconstruction in EIT

The goal of EIT image reconstruction is to obtain the conductivity image of an object's interior, with the type of reconstruction algorithm determining image quality [45], [128]. Common techniques used in the reconstruction process include finite element method-based forward problems, iterative regularization, and machine learning approaches [129]. The forward problem involves constructing a digital model [120] and sensitivity matrix (Jacobian) for the inverse solver [130]. Correspondingly, the inverse problem aims to determine the conductivity distribution using the boundary voltage difference vector and sensitivity matrix [130]. However, the inverse problem, being ill-posed and non-linear, requires linearization and regularization or sophisticated algorithms for accurate image reconstruction [37]. Kalman filters and smoothing approaches in time-varying EIT reconstruction problems significantly enhance temporal resolution compared to traditional methods [118], [131]. Dynamic imaging techniques further improve temporal resolution of reconstructed images when resistivity distribution changes rapidly [131]. Kim et al. [132] proposed using an extended Kalman filter and Tikhonov regularization to enhance spatial and temporal resolution in the resistivity distribution. A number of algorithms are available in EIDORS software for reconstructing electrical conductivity [115], [127], [133]. Darma and Takei suggested using the k-nearest

Accepted Manuscript

neighbour algorithm to approximate the Jacobian matrix and improve reconstruction speed [134].

Despite advancements in regularization methods for solving the EIT inverse problem, image reconstruction accuracy remains low, and computation time is long. However, machine learning and advanced filtering methods have significantly improved both accuracy and computation time [135]. Impedance data is transformed into features using methods like principal component analysis (PCA) or time-frequency analysis, then input into classifiers like SVMs, neural networks, or decision trees to identify activities [48], [136]. Pessoa et al. [135] showed that combining EIT data processing and feature engineering with machine learning models can develop differential diagnosis systems. A recent review article revealed that combining traditional algorithms with deep learning and DNN hybrid strategies offers greater advantages in EIT image reconstruction [129]. Additionally, convolutional neural networks (CNNs) have shown strong performance in addressing EIT inverse problem challenges by capturing spatial features, reconstructing intricate tissue conductivity patterns, and improving robustness against noise [46], [128]. Recent advances in different image reconstruction techniques and developments have also been reviewed [120].

EIT's portability, safety, and continuous monitoring make it ideal for activity recognition tasks. Devices like Maltron Sheffield MK 3.5, LuMonTM System, and PulmoVista 500 are notable for muscle activation, respiratory monitoring, breast cancer detection, and geophysical exploration [37], [117].

3. Applications of Bioimpedance Technology systems

Bioimpedance technology systems have demonstrated increasing utility across various domains due to their ability to non-invasively measure and analyse the electrical properties of biological tissues. These systems provide valuable insights into physiological parameters and are widely applied in activity-based monitoring contexts. Table 4 presents a concise summary of the application areas where bioimpedance technologies have been employed for activity-related measurements.

Table 4: Summary of bioimpedance technology applications in activity monitoring

Applications	Descriptions	Bioimpedance modality	Ref
Muscle activity/health monitoring	Measuring electrical or mechanical signals from muscles to assess their function.	EIM	[137] [138] [139]
Rehabilitation assessment	Evaluating a patient's physical function and recovery progress.	EIT	[140] [115]
		EIM	[101] [141] [142]
Muscle fatigue monitoring during exercise	Tracks changes in muscle electrical signals to assess performance decline and endurance in real time.	MF-BIA	[143] [144] [145]
		EIM	[146] [147] [148] [149] [150] [151]
Muscle contractions for prosthesis regulation	Detecting electrical signals from muscles to control the movements of an artificial limb.	EIM	[99] [152] [153]
Gesture recognition	Identifying and interpreting hand or body gestures using sensors.	EIT	[45] [46] [154] [47] [56] [136] [155]

Accepted Manuscript

Neuromuscular assessment	Evaluation of muscle and nerve function to identify, monitor, or diagnose neuromuscular disorders	EIM	[57] [156] [157] [158] [159] [160]
Respiratory monitoring	Measurement of breathing patterns, rate, and volume to assess lung function and detect respiratory abnormalities	EIM	[36] [120] [130] [161] [162]

3.1. Muscle Activity Monitoring

Bioimpedance systems effectively monitor the impact of electrical stimulation on muscle cells. Nevertheless, Bailleul et al. [137] designed a platform integrating bioimpedance spectroscopy, electrical stimulation, and optical microscopy for real-time monitoring, revealing that bioimpedance decreases with increased duration or frequency of electrical stimulation. Due to the limitations of electromyography in detecting passive muscle movement, Kusche et al. [139] developed a wearable and portable dual channel bioimpedance spectrometer to detect real-time muscle contractions, showing frequency-dependent phase changes. Hornero et al. [163] combined electrical impedance myography (EIM) and electrical impedance plethysmography (IPG) to monitor muscle and cardiovascular activity in lower-limb amputees, accurately measuring muscle activity, heart and breathing rates. Moreover, EIM technique has also been used to analyse muscle activity during physical activities, with devices (Max30009EVKIT and Max86178EVKIT) showing unique signal characteristics for different activities and individual variations in muscle activation patterns [138] (see figure 16).

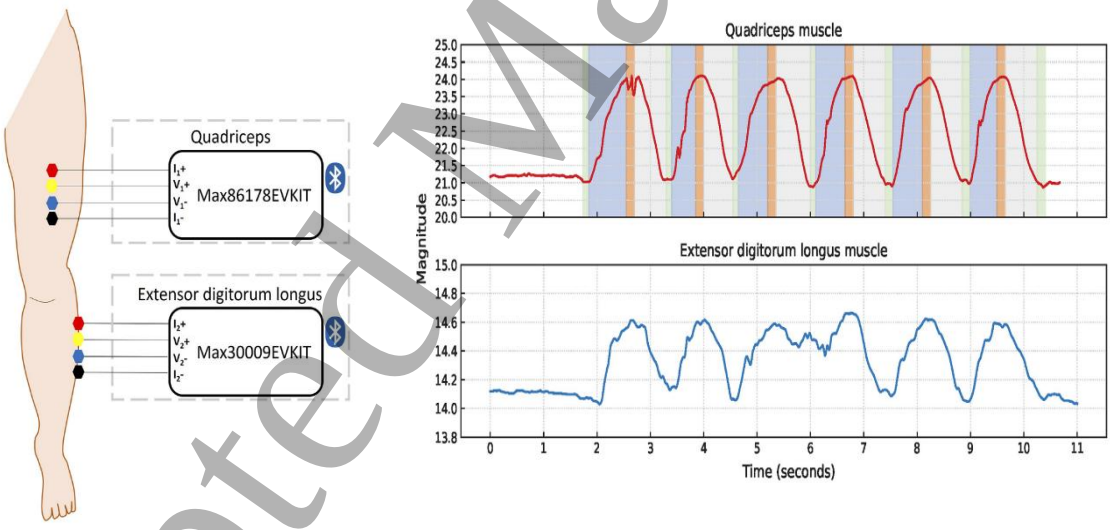

Fig. 16: Experimental setup of Max30009EVKIT and Max86178EVKIT with Ag/AgCl gel electrodes. Reproduced from Hafid et al. [138]

Studies have shown that EIT can be utilized in muscle health assessment. For example, Patil et al. [140] found that using EIT to monitor muscle activity during robot-assisted rehabilitation improves rehabilitation outcomes compared to traditional EMG, allowing for better monitoring and more personalized treatments. Additionally, Zhu et al. [115] developed a personal muscle monitor for sensing thigh muscle strain and tension to aid recovery and prevent re-injury. A recent study has reported that combining ultrasound with EIT improves image accuracy and captures comprehensive muscle characteristics [39].

Accepted Manuscript

3.2. Fatigue and Fitness Monitoring

Monitoring muscle fatigue and exercise fitness is crucial for optimizing athletic performance, preventing injuries, and guiding rehabilitation. Traditional methods such as ultrasound imaging, muscle biopsies, and motion capture systems are restricted to clinical settings and not feasible for everyday use [143]. Neuromuscular fatigue results from complex interactions between central and peripheral mechanisms, leading to reduced muscle force production [164]. However, a muscle fatigue digital biomarker, termed "fatigue score," derived from dual frequency bioimpedance analysis (DFBIA) signal estimates the percentage reduction in muscle force during exercise with a high accuracy [143]. Furthermore, Vescio et al. [144] validated that multifrequency bioimpedance measurements effectively monitor muscle fatigue by detecting impedance changes.

Various studies have employed bioimpedance technology to monitor and detect changes in muscle fibres before, during and after exercise in real-time [147]. Huang et al. [146] used EIM to monitor muscle fatigue during dynamic contractions, finding significant resistance decreases. They concluded that this method is feasible, efficient, and suitable for wearable devices. Furthermore, Zhou et al. [149] evaluated muscle fatigue induced by neuromuscular electrical stimulation (NMES) in real-time using EIM, focusing on impedance amplitude and phase angle. They found that both parameters decrease significantly during NMES within 20 kHz–150 kHz frequencies, with high-frequency NMES inducing fatigue faster than low-frequency NMES. Due to the sensitivity of localized bicep tissue bioimpedance to capture tissue changes during eccentric exercise, Freeborn et al. [148] compared muscle changes in exercised and non-exercised arms, finding a significant impedance decrease in the exercised arm at different frequencies. Furthermore, Yamaguchi et al. [145] used multi-frequency BIA to assess muscle tissue status during exercise-induced muscle damage, finding greater intra- and extracellular water content, and lower impedance, reactance, resistance, and phase angle in the exercised arm compared to the control arm at all time.

An investigation by Freeborn and Fu [150] reported that the Cole electrical impedance model effectively captures exercise-induced fatigue changes in biceps tissue bioimpedance, especially in resistance components. However, a study on EIM of the biceps brachii muscle found that resistance increases significantly at higher isometric contraction levels and decreases with muscle fatigue, with no significant changes in reactance [151]. Shiffman et al. [165] found that EIM measurements of muscle impedance during isometric contractions agree with Li et al. [151] on resistance behaviour but disagree on reactance.

Studies show that electromyography (EMG) is commonly used to detect muscle contractions but is sensitive to mechanical disturbances. However, Kusche and Ryschka [99] suggested that combining EMG with bioimpedance measurements enhances the reliability and accuracy of muscle contraction detection, which is beneficial for prosthetic control and other applications. Consequently, mechanical disturbances (motion artifacts) cause more negative phase shifts in measured reactance. The PhaseX Effect method, proposed to improve muscle contraction detection using multi-frequency impedance myography, offers higher reliability and lower signal processing requirements compared to traditional EMG [152]. To further improve the

Accepted Manuscript

reliability of muscle contraction detection, Yakim et al. [153] developed a real-time signal processing system using electrical impedance measurements, effectively and reliably detecting muscle contractions without auxiliary switches.

3.3. Gesture Recognition

Human gestures, like hand and finger movements, cause muscle contractions and blood flow changes, affecting tissue conductivity. Recent studies show that electrical impedance tomography can capture these changes and use them for real-time gesture recognition by injecting a small current and measuring voltage patterns [45], [47], [56], [155]. Researchers have applied deep/machine learning algorithms in EIT to recognize and classify human activities as shown in figure 17 [46]. Atitallah et al. [166] investigated hand sign recognition system using electrical impedance tomography (EIT) and a convolutional neural network (CNN) classification. Their proposed system showed low complexity, achieving high classification accuracy and robustness in hand sign recognition. Gibas et al. [155] created a mobile wearable EIT system for detecting extremity muscle activity, showing reproducible gesture detection.

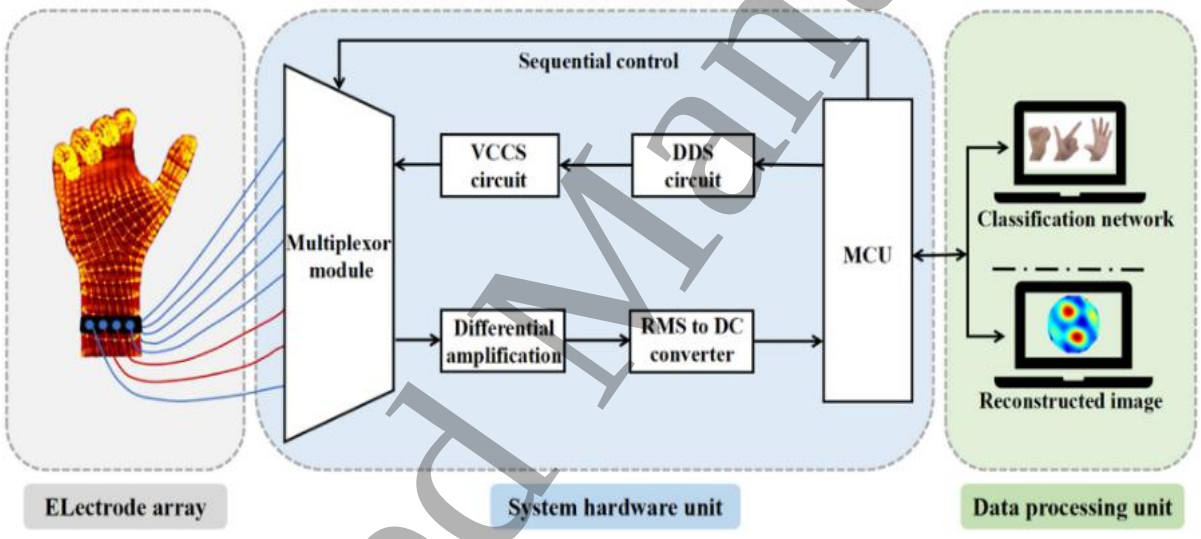

Fig.17: The overall structures of the EIT system for gesture classification. Reproduced from Li et al. [46].

Furthermore, Vaquero-Gallardo and Martínez-García [154] explored using electrical impedance tomography for hand gesture recognition in HMI applications. They used principal component analysis (PCA) to reduce data into three patterns (A, B, and C), with the k-nearest neighbour algorithm achieving high classification accuracy, and pattern C being the optimal pattern. A recent study developed a wearable EIT sensor for gesture recognition, achieving high accuracy with the rectangular copper electrodes and using the Gaussian SVM algorithm in MATLAB's machine learning toolbox [56]. The findings emphasize the importance of electrode material, shape, and contact impedance in optimizing gesture recognition systems.

Research has shown that dynamic gestures, when compared to static gestures, are complex but more informative and can achieve more functions in human-machine collaboration. Li et al. [46] introduced CG-SVM, a dual-channel feature extraction network that integrates CNN and

Accepted Manuscript

gated recurrent unit (GRU) to enhance dynamic gesture recognition accuracy. By optimizing the excitation current drive pattern, their classification network significantly improves recognition accuracy amidst different interference data. Table 5 shows a summary of previous studies on gesture recognition using bioimpedance techniques.

Table 5: Summary of Studies on Gesture Recognition using EIT Measurement

Author(s)	No of Electrode	No of Gesture	Subjects	Reconstruction Algorithm	Classification Models	Findings
Zhang et al. [45]	8, 16 and 32	11	10	Nodal one-step Gauss-Newton iterative solver: maximum a posteriori (MAP) estimator	Support vector machine (SVM) with a Polynomial kernel	Four-pole, 32 electrodes achieved the best accuracy of 94.3% for the combined gesture set.
Li et al. [46]	8 and 16	5	5	Nil	CNN and GRU integrated in SVM (CGSVM), CNN and SVM	CG-SVM3 network outperformed the SVM algorithm and CNN network
Vaquero-Gallardo and Martínez-García [154]	8	6	1	Nil	Principal Component Analysis (PCA), k-nearest neighbor (kNN)	kNN achieves high sensitivity values (above 0.89) for k = 6, among the reduced patterns
Zhang and Harrison [47]	8	Pinch gesture = 4, Hand gesture = 7	10	Linear Back Projection (LBP)	Support vector machine (SVM) with a Polynomial kernel	Accuracy: Wrist location (hand = 97%, Pinch = 87%). Arm location (hand = 93%, Pinch = 81%)
Yao et al [56]	8	3	6	Generalized Vector Sampled Pattern Matching algorithm	Medium Gaussian SVM, Bagged Trees Ensemble, and Quadratic Discriminant	Medium Gaussian SVM algorithm gave optimal recognition average accuracy of 95%.
Jiang et al. [123]	16	8	1	Not reported	Decision trees, Support vector machines and Artificial neural networks	3D EIT arrangement achieves 98.25% accuracy while 2D EIT system achieved 97%
Leins et al. [121]	16	12	1	Nil	Convolutional neural networks (CNNs) and dual-input networks	Calibration methods increased classification accuracy to 39.01%, 55.37%, and 56.34%.
Lu et al. [136]	8	9	1	Tikhonov regularization	Quadratic Discriminant (QD), Quadratic Support Vector Machine (QSVM), Linear Discriminant (LD).	Recognition accuracy: QD = 98.49%, QSVM = 98.16%, and LD = 97.99%,

Accepted Manuscript

Gibas et al. [155]	16	10	5	Graz consensus Reconstruction algorithm for EIT (GREIT) software from EIDORS	No Classification	Best reconstructed image achieved at 100kHz and 5mA. Some gestures were more reproducible than others.
Atitallah et al. [166]	8	10	8	Gauss-Newton image reconstruction algorithm	CNN, Support Vector Machine and Softmax classifiers	Classification accuracy (%): CNN = 95.94, SVM = 75.61 and Softmax = 62.9

3.4 Other bioimpedance measurement applications:

In addition to its applications in human activity recognition, bioimpedance measurement technology has been increasingly explored for its utility in a range of physiological monitoring contexts. Notably, it plays a critical role in the assessment and management of neuromuscular disorders, as well as in non-invasive monitoring of respiratory functions.

3.4.1. Neuromuscular disorders

Bioimpedance technology, especially electrical impedance myography (EIM), is a valuable tool for assessing and managing neuromuscular diseases. It is widely used as a diagnostic tool and biomarker for disease progression in both human and animal studies [57], [101]. Despite its challenges, various studies have used it to diagnose and monitor neuromuscular disorders [156], [157]. However, Alix et al. [158] demonstrated that multi-dimensional EIM of the tongue can reliably distinguish amyotrophic lateral sclerosis (ALS) patients from healthy individuals and detect disease progression (bulbar dysfunction) over time. Moreover, EIM effectively quantifies muscle inflammation induced by localized intramuscular injection of λ-carrageenan, eliminating the need for a biopsy [167]. A systematic review by Cebrián-Ponce et al. [168] highlights EIM's potential as an alternative to traditional muscle assessment tools like MRI. However, it emphasizes the need for standardized measurement protocols and further research to validate its clinical and sports applications. Additionally, Gong et al. [141] proposed integrating EIM with techniques like ultrasonography, MRI, CT, myotonometry, and machine learning to improve the assessment of stroke-related muscle dysfunction, enhancing diagnostic accuracy and rehabilitation outcomes.

The use of quantitative muscle ultrasound and EIM as biomarkers for monitoring muscle health in Late-Onset Pompe Disease (LOPD) has been explored. Results show that handheld EIM is reliable, feasible for home or remote monitoring, and can detect early muscle disease [159]. An investigation on EIM assessment of muscles in patients with incomplete cervical spinal cord injury (SCI) shows that EIM can be used in clinical settings to examine neuromuscular health and guide rehabilitation strategies [102], [142]. Rosa-Caldwell et al. [169] found that combining EIM with machine learning can predict muscle mass and function in rat models in micro and partial gravity environments. This non-invasive tool could help monitor muscle changes and assess astronaut muscle health during space missions. Conversely, Sanchez et al. [160] demonstrated that EIM can non-invasively detect skeletal muscle alterations associated with injury in both healthy and dystrophic animals. Correspondingly, Rutkove et al. [170] found that EIM methods can detect and quantify skeletal muscle function in adult zebrafish.

Accepted Manuscript

3.4.2. Respiratory Monitoring

Electrical impedance tomography (EIT) is widely used to monitor respiratory and cardiac activity, providing real-time lung function insights that guide precise ventilation adjustments and therapeutic interventions [130]. Consequently, it uses high-frequency, low-amplitude alternating electrical currents through a 16 or 32 electrode array around the thorax to obtain cross-sectional lung images [120]. An open-source EIT system for monitoring the lungs of free-breathing subjects has been developed and tested in a phantom [36], performing similarly to commercial devices. Furthermore, a portable EIT system developed for real-time respiratory monitoring shows good correlations between instantaneous respiratory rate and tidal volume prediction [161]. Schullcke et al. [162] utilized EIT to monitor disease progression in patients with obstructive lung diseases like chronic obstructive pulmonary disease and cystic fibrosis, providing comprehensive insights into lung pathophysiology. Recent studies show that AI integration enhances EIT diagnostic capabilities, leading to more accurate, user-friendly devices and personalized treatment plans [130], [171]. Moreover, a narrative review on the methodologies and applications of electrical impedance tomography in lung diseases with flow limitation and hyperinflation has been reported [172].

4. Limitations and Challenges of EIT and EIM Systems

Despite offering valuable insights into physiological parameters, bioimpedance devices still face limitations and challenges in measurement techniques. For example, although EIT provides good temporal resolution and enables real-time monitoring, its spatial resolution remains comparatively low relative to other imaging modalities. This limitation reduces its capacity to distinguish between spatially similar human activities, as subtle impedance variations may be blurred during reconstruction [45]. Consequently, real-time activity recognition requires fast and efficient image reconstruction and classification algorithms [56]. So, balancing accuracy and computational efficiency are crucial. The inverse problem of recovering conductivity distribution is ill-posed due to nonlinearity and low sensitivity, making it computationally intensive [127], [166]. The NOSER and back projection algorithms are fast in computation but less accurate due to their simplified assumptions, limited iterations, and sensitivity to noise and incomplete data [116], [173], [174]. Also, frequency interference affects EIT signal quality when using with other bioimpedance systems [39].

Furthermore, studies report that obtaining accurate boundary geometry and electrode positions is challenging, making the inverse problem sensitive to modelling errors, measurement artifacts and noise particularly during dynamic tasks. This results in poor spatial resolution [175]. However, the reconstruction of high-resolution images and modelling the geometry in real-time remain difficult for portable EIT systems [119]. Also, variations in electrode contact, configuration, and motion artifacts pose significant challenges, especially in wearable applications [126]. Several studies show a lack of standardization in electrode placement and configuration in EIM, leading to varying accuracies and hindering clinical adoption [104], [156]. Additionally, the difficulty in collecting large, high-quality datasets limits the training of machine learning models, making the integration of bioimpedance technology with medical

Accepted Manuscript

technologies challenging [130]. As a result of these limitations, most studies lack quantified data for statistically analysing sources of error inherent in reported applications.

Wang et al. [176] address limitations of traditional EIM systems by redesigning and validating electrode configurations, enabling more accurate and compact wearable muscle monitoring. Sanchez et al. [177] enhance EIM reliability and reproducibility through a standardized framework for electrode placement applicable to both human and animal models. Furthermore, Sanchez et al. [100] propose needle EIM as a significant advancement in neuromuscular diagnostics, offering high-resolution, artifact-resistant measurements that overcome the constraints of surface EIM. Complementing these advancements, Sanchez and Rutkove [57] outline a comprehensive set of solutions including optimized electrode configuration via computational modelling, improved electrode materials and placement protocols, real-time impedance monitoring, impedance imaging, and integration into wearable and telehealth platforms.

5. Emerging Trends and Recent Advances

Despite the challenges such as inaccuracy, advancements in hybrid sensor technology, artificial intelligence integration, and clinical validation can improve the reliability and utility of bioimpedance devices, making detailed body assessments more reliable.

5.1. Hybrid Modalities

Bioimpedance measurement are technologies compatible with other sensing technologies like electromyography (EMG) [99], [178], ultrasound (US) [179], [180] or magnetic resonance imaging (MRI) [175] and combining these modes enhances image accuracy and robustness. Multimodal systems, like acoustic-electric impedance tomography (aEIT), which combines ultrasound and electrical impedance measurements, are increasingly popular for creating images based on tissue conductivity changes [128]. Woo and Seo [175] explored using magnetic resonance electrical impedance tomography (MREIT) for high-resolution conductivity imaging. This involves using an MRI scanner to measure internal magnetic flux density with externally injected currents, which can cause injury if not regulated. Moreover, Ngo et al. [181] developed a wearable, multi-frequency device combining EMG and EIM to enhance muscle activity measurement and force estimation for robot-assisted rehabilitation. The device achieved accurate and reliable measurements with less than 100 ms delay between signals. A study by Liu et al. [182] demonstrated that bio-impedance can enhance IMU-based tracking through sensor fusion and contrastive learning, achieving higher accuracy in recognizing fitness activities.

5.2. Wearable and Portable Systems

Wearable bioimpedance devices provide real-time body impedance data, improving at-home monitoring and reducing clinical visits. The use of large electrodes to minimize contact impedance is a challenge for wearable devices [183]. Subsequently, advances in flexible electronics and miniaturized hardware are enabling the development of wearable, lightweight, portable bioimpedance systems for continuous activity monitoring in real-world settings [184]. Zhang et al. [129] designed a flexible, skin-conformal EIT sensor array for monitoring limb

Accepted Manuscript

movements, achieving high accuracy in classifying basic activities such as arm lifting and leg bending. However, Zhang and Harrison [47] also developed a lightweight, low-cost wearable EIT for gesture detection, with high accuracy in gross hand gestures and thumb-to-finger pinches. Moreover, Kusche et al. [139] designed a wearable, real-time bioimpedance spectrometer for muscle contraction detection that can record the frequency responses in the range of 20 to 230 kHz from two antagonistic muscles, whereas Lu et al. [136] developed a low-cost, wearable gesture recognition system using the two-electrode terminal EIT technique.

A recent study introduced a flexible, lattice-patterned EIT-based tactile sensor for tactile sensing applications. This wearable EIT system offers comfortable, non-intrusive monitoring and achieves high spatial resolution with a hydrogel-based conductive layer [185]. Furthermore, a rectangular copper electrode amongst conductive cloth, curved copper and medical electrode has been employed in the development of a wearable electrode-skin contact EIT device for gesture recognition due to its high recognition rate [56].

Many studies have integrated machine learning models into wearable bioimpedance systems. Cornelius et al. [186] designed a portable system that uses Naive Bayes and Support Vector Machine classifiers for human identification and verification. The challenges of integrating bioimpedance sensors into wearable devices, focusing on portability, comfort, hardware miniaturization, electrode design, power consumption, and measurement optimization have been discussed here [187], [188].

6. Conclusion

This article provides a scoping review of bioimpedance technology, focusing on its basic principles, diverse applications, and recent advancements in human activity recognition. Bioimpedance measurement is a non-invasive, cost-effective technique that has undergone significant evolution, offering real-time monitoring of physiological parameters and human activities. The review highlights various bioimpedance measurement methods, including Bioelectrical Impedance Analysis (BIA), Electrical Impedance Myography (EIM), and Electrical Impedance Tomography (EIT), each with unique advantages and applications.

Despite inherent challenges such as low spatial resolution, lack of standardized protocols, and sensitivity to electrode placement, the field is rapidly advancing. Innovations in hybrid sensor systems, integration with artificial intelligence models, and the development of wearable and flexible electronics are enhancing the accuracy, reliability, and usability of bioimpedance devices. These improvements are expanding the technology's potential across domains such as personalized healthcare, fitness tracking, rehabilitation, and human-machine interaction.

The article also discusses recent advancements in bioimpedance technology that address key challenges such as measurement inaccuracies and sensitivity to electrode placement. Through the integration of hybrid sensor modalities, artificial intelligence, and wearable systems, these innovations are enhancing the reliability and accuracy of bioimpedance measurements, making them increasingly viable for real-world applications.

References

Accepted Manuscript

[1] M. Hargreaves and L. L. Spriet, "Skeletal muscle energy metabolism during exercise," *Nat. Metab.*, vol. 2, no. 9, pp. 817–828, Aug. 2020, doi: 10.1038/s42255-020-0251-4.

[2] V. Škop *et al.*, "The metabolic cost of physical activity in mice using a physiology-based model of energy expenditure," *Mol. Metab.*, vol. 71, p. 101699, May 2023, doi: 10.1016/j.molmet.2023.101699.

[3] P. C. Hallal, L. B. Andersen, F. C. Bull, R. Guthold, W. Haskell, and U. Ekelund, "Global physical activity levels: surveillance progress, pitfalls, and prospects," *The Lancet*, vol. 380, no. 9838, pp. 247–257, July 2012, doi: 10.1016/S0140-6736(12)60646-1.

[4] N. Hnoohom, S. Mekruksavanich, and A. Jitpattanakul, "Physical Activity Recognition Based on Deep Learning Using Photoplethysmography and Wearable Inertial Sensors," *Electronics*, vol. 12, no. 3, p. 693, Jan. 2023, doi: 10.3390/electronics12030693.

[5] I. A. Bustoni, I. Hidayatulloh, A. M. Ningtyas, A. Purwaningsih, and S. N. Azhari, "Classification methods performance on human activity recognition," *J. Phys. Conf. Ser.*, vol. 1456, no. 1, p. 012027, Jan. 2020, doi: 10.1088/1742-6596/1456/1/012027.

[6] A. Hayat, F. Morgado-Dias, B. Bhuyan, and R. Tomar, "Human Activity Recognition for Elderly People Using Machine and Deep Learning Approaches," *Information*, vol. 13, no. 6, p. 275, May 2022, doi: 10.3390/info13060275.

[7] X. Yin, Z. Liu, D. Liu, and X. Ren, "A Novel CNN-based Bi-LSTM parallel model with attention mechanism for human activity recognition with noisy data," *Sci. Rep.*, vol. 12, no. 1, p. 7878, May 2022, doi: 10.1038/s41598-022-11880-8.

[8] F. Demrozi, G. Pravadelli, A. Bihorac, and P. Rashidi, "Human Activity Recognition using Inertial, Physiological and Environmental Sensors: a Comprehensive Survey," *IEEE Access*, vol. 8, pp. 210816–210836, 2020, doi: 10.1109/ACCESS.2020.3037715.

[9] U. Zia, W. Khalil, S. Khan, I. Ahmad, and M. N. Khan, "Towards human activity recognition for ubiquitous health care using data from awaist-mounted smartphone," *Turk. J. Electr. Eng. Comput. Sci.*, vol. 28, no. 2, pp. 646–663, Mar. 2020, doi: 10.3906/elk-1901-31.

[10] U. Oleh, R. Obermaisser, and A. S. Ahammed, "A Review of Recent Techniques for Human Activity Recognition: Multimodality, Reinforcement Learning, and Language Models," *Algorithms*, vol. 17, no. 10, p. 434, Sept. 2024, doi: 10.3390/a17100434.

[11] Y. Wang, S. Cang, and H. Yu, "A survey on wearable sensor modality centred human activity recognition in health care," *Expert Syst. Appl.*, vol. 137, pp. 167–190, Dec. 2019, doi: 10.1016/j.eswa.2019.04.057.

[12] Z. Yu *et al.*, "An Intelligent Implementation of Multi-Sensing Data Fusion With Neuromorphic Computing for Human Activity Recognition," *IEEE Internet Things J.*, vol. 10, no. 2, pp. 1124–1133, Jan. 2023, doi: 10.1109/JIOT.2022.3204581.

[13] L. Zhang, J. Yu, Z. Gao, and Q. Ni, "A multi-channel hybrid deep learning framework for multi-sensor fusion enabled human activity recognition," *Alex. Eng. J.*, vol. 91, pp. 472–485, Mar. 2024, doi: 10.1016/j.aej.2024.01.030.

[14] Y. Chen and C. Shen, "Performance Analysis of Smartphone-Sensor Behavior for Human Activity Recognition," *IEEE Access*, vol. 5, pp. 3095–3110, 2017, doi: 10.1109/ACCESS.2017.2676168.

[15] M. Shoaib, H. Scholten, and P. J. M. Havinga, "Towards Physical Activity Recognition Using Smartphone Sensors," in *2013 IEEE 10th International Conference on Ubiquitous Intelligence and Computing and 2013 IEEE 10th International Conference on Autonomic and Trusted Computing*, Italy: IEEE, Dec. 2013, pp. 80–87. doi: 10.1109/UIC-ATC.2013.43.

[16] U. Saha, S. Saha, T. Kabir, S. A. Fattah, and M. Saquib, "Decoding Human Activities: Analyzing Wearable Accelerometer and Gyroscope Data for Activity Recognition," July 08, 2024, *arXiv*: arXiv:2310.02011. Accessed: Nov. 01, 2024. [Online]. Available: http://arxiv.org/abs/2310.02011

[17] J. R. Kwapisz, G. M. Weiss, and S. A. Moore, "Activity recognition using cell phone accelerometers," *ACM SIGKDD Explor. Newsl.*, vol. 12, no. 2, pp. 74–82, Mar. 2011, doi: 10.1145/1964897.1964918.

[18] M. Kołodziej and K. Czajka, "Skeletal muscle quality in 6- and 7-y-old children assessed using bioelectrical impedance analysis," *Nutrition*, vol. 96, p. 111568, Apr. 2022, doi: 10.1016/j.nut.2021.111568.

Accepted Manuscript

[19] G. Anand, Y. Yu, A. Lowe, and A. Kalra, "Bioimpedance analysis as a tool for hemodynamic monitoring: overview, methods and challenges," *Physiol. Meas.*, vol. 42, no. 3, p. 03TR01, Mar. 2021, doi: 10.1088/1361-6579/abe80e.

[20] J. Qi, P. Yang, G. Min, O. Amft, F. Dong, and L. Xu, "Advanced internet of things for personalised healthcare systems: A survey," *Pervasive Mob. Comput.*, vol. 41, pp. 132–149, Oct. 2017, doi: 10.1016/j.pmcj.2017.06.018.

[21] A. Gupta, K. Gupta, K. Gupta, and K. Gupta, "A Survey on Human Activity Recognition and Classification," in *2020 International Conference on Communication and Signal Processing (ICCSP)*, Chennai, India: IEEE, July 2020, pp. 0915–0919. doi: 10.1109/ICCSP48568.2020.9182416.

[22] Z. Hussain, M. Sheng, and W. E. Zhang, "Different Approaches for Human Activity Recognition: A Survey," *J. Netw. Comput. Appl.*, vol. 167, p. 102738, Oct. 2020, doi: 10.1016/j.jnca.2020.102738.

[23] F. Kulsoom, S. Narejo, Z. Mehmood, H. N. Chaudhry, A. Butt, and A. K. Bashir, "A review of machine learning-based human activity recognition for diverse applications," *Neural Comput. Appl.*, vol. 34, no. 21, pp. 18289–18324, Nov. 2022, doi: 10.1007/s00521-022-07665-9.

[24] A. A. Aguileta, R. F. Brena, O. Mayora, E. Molino-Minero-Re, and L. A. Trejo, "Multi-Sensor Fusion for Activity Recognition—A Survey," *Sensors*, vol. 19, no. 17, p. 3808, Sept. 2019, doi: 10.3390/s19173808.

[25] H. F. Nweke, Y. W. Teh, G. Mujtaba, and M. A. Al-garadi, "Data fusion and multiple classifier systems for human activity detection and health monitoring: Review and open research directions," *Inf. Fusion*, vol. 46, pp. 147–170, Mar. 2019, doi: 10.1016/j.inffus.2018.06.002.

[26] P. Xu *et al.*, "Advancements and Challenges in Electrical Impedance Myography (EIM): A Comprehensive Overview of Technology Development, Applications in Sports Health, and Future Directions," *IEEE J. Microw.*, vol. 4, no. 4, pp. 605–625, Oct. 2024, doi: 10.1109/JMW.2024.3427710.

[27] M. S. D. Awachar, D. D. T. Ingole, and M. D. Ingole, "A Review Paper on Human Activity Recognition Using Smart Phone Sensors," *Int. J. Creat. Res. Thoughts*, vol. 6, no. 1, pp. 594–598, 2018.

[28] C. Contoli, V. Freschi, and E. Lattanzi, "Energy-aware human activity recognition for wearable devices: A comprehensive review," *Pervasive Mob. Comput.*, vol. 104, p. 101976, Nov. 2024, doi: 10.1016/j.pmcj.2024.101976.

[29] P. Kumar, S. Chauhan, and L. K. Awasthi, "Human Activity Recognition (HAR) Using Deep Learning: Review, Methodologies, Progress and Future Research Directions," *Arch. Comput. Methods Eng.*, vol. 31, no. 1, pp. 179–219, Jan. 2024, doi: 10.1007/s11831-023-09986-x.

[30] G. Saleem, U. I. Bajwa, and R. H. Raza, "Toward human activity recognition: a survey," *Neural Comput. Appl.*, vol. 35, no. 5, pp. 4145–4182, Feb. 2023, doi: 10.1007/s00521-022-07937-4.

[31] Y. Yu, A. Lowe, G. Anand, A. Kalra, and H. Zhang, "The Investigation of Bio-impedance Analysis at a Wrist Phantom with Two Pulsatile Arteries," *Cardiovasc. Eng. Technol.*, vol. 14, no. 6, pp. 810–826, Dec. 2023, doi: 10.1007/s13239-023-00689-9.

[32] H. Zhang, A. Kalra, A. Lowe, Y. Yu, and G. Anand, "A Hydrogel-Based Electronic Skin for Touch Detection Using Electrical Impedance Tomography," *Sensors*, vol. 23, no. 3, p. 1571, Feb. 2023, doi: 10.3390/s23031571.

[33] S. El Dimassi, J. Gautier, V. Zalc, S. Boudaoud, and D. Istrate, "Body Water Volume Estimation Using Bio Impedance Analysis: Where Are We?" *IRBM*, vol. 45, no. 3, p. 100839, June 2024, doi: 10.1016/j.irbm.2024.100839.

[34] H. Arksey and L. O'Malley, "Scoping studies: towards a methodological framework," *Int. J. Soc. Res. Methodol.*, vol. 8, no. 1, pp. 19–32, Feb. 2005, doi: 10.1080/1364557032000119616.

[35] N. R. Haddaway, M. J. Page, C. C. Pritchard, and L. A. McGuinness, "*PRISMA2020*: An R package and Shiny app for producing PRISMA 2020-compliant flow diagrams, with interactivity for optimised digital transparency and Open Synthesis," *Campbell Syst. Rev.*, vol. 18, no. 2, p. e1230, June 2022, doi: 10.1002/cl2.1230.

[36] A. Creegan *et al.*, "A Wearable Open-Source electrical impedance tomography device," *HardwareX*, vol. 18, p. e00521, June 2024, doi: 10.1016/j.ohx.2024.e00521.

Accepted Manuscript

[37] Z. Zheng, Z. Wu, R. Zhao, Y. Ni, X. Jing, and S. Gao, "A Review of EMG-, FMG-, and EIT-Based Biosensors and Relevant Human–Machine Interactivities and Biomedical Applications," *Biosensors*, vol. 12, no. 7, p. 516, July 2022, doi: 10.3390/bios12070516.

[38] Y. Moshkovitz, E. Kaluski, O. Milo, Z. Vered, and G. Cotter, "Recent developments in cardiac output determination by bioimpedance: comparison with invasive cardiac output and potential cardiovascular applications:," *Curr. Opin. Cardiol.*, vol. 19, no. 3, pp. 229–237, May 2004, doi: 10.1097/00001573-200405000-00008.

[39] F. Pennati *et al.*, "Electrical Impedance Tomography: From the Traditional Design to the Novel Frontier of Wearables," *Sensors*, vol. 23, no. 3, p. 1182, Jan. 2023, doi: 10.3390/s23031182.

[40] L. C. Ward and S. Brantlov, "Bioimpedance basics and phase angle fundamentals," *Rev. Endocr. Metab. Disord.*, vol. 24, no. 3, pp. 381–391, June 2023, doi: 10.1007/s11154-022-09780-3.

[41] A. Prasad and M. Roy, "Bioimpedance analysis of vascular tissue and fluid flow in human and plant body: A review," *Biosyst. Eng.*, vol. 197, pp. 170–187, Sept. 2020, doi: 10.1016/j.biosystemseng.2020.06.006.

[42] S. F. Scagliusi *et al.*, "Bioimpedance Spectroscopy-Based Edema Supervision Wearable System for Noninvasive Monitoring of Heart Failure," *IEEE Trans. Instrum. Meas.*, vol. 72, pp. 1–8, 2023, doi: 10.1109/TIM.2023.3273662.

[43] A. M. Kalra, G. Anand, A. Lowe, R. Simpkin, and D. Budgett, "A smart idea to reject motion artefacts from ECG measurements due to sensor-body impedance".

[44] A. Ivorra *et al.*, "Bioimpedance dispersion width as a parameter to monitor living tissues," *Physiol. Meas.*, vol. 26, no. 2, pp. S165–S173, Apr. 2005, doi: 10.1088/0967-3334/26/2/016.

[45] Y. Zhang, R. Xiao, and C. Harrison, "Advancing Hand Gesture Recognition with High Resolution Electrical Impedance Tomography," in *Proceedings of the 29th Annual Symposium on User Interface Software and Technology*, Tokyo Japan: ACM, Oct. 2016, pp. 843–850. doi: 10.1145/2984511.2984574.

[46] X. Li *et al.*, "Dynamic Hand Gesture Recognition Using Electrical Impedance Tomography," *Sensors*, vol. 22, no. 19, p. 7185, Sept. 2022, doi: 10.3390/s22197185.

[47] Y. Zhang and C. Harrison, "Tomo: Wearable, Low-Cost Electrical Impedance Tomography for Hand Gesture Recognition," in *Proceedings of the 28th Annual ACM Symposium on User Interface Software & Technology*, Charlotte NC USA: ACM, Nov. 2015, pp. 167–173. doi: 10.1145/2807442.2807480.

[48] N. Vaquero-Gallardo and H. Martínez-García, "Electrical Impedance Tomography for Hand Gesture Recognition for HMI Interaction Applications," *J. Low Power Electron. Appl.*, vol. 12, no. 3, p. 41, July 2022, doi: 10.3390/jlpea12030041.

[49] P. Bogónez-Franco, L. Nescolarde, R. Bragós, J. Rosell-Ferrer, and I. Yandiola, "Measurement errors in multifrequency bioelectrical impedance analyzers with and without impedance electrode mismatch," *Physiol. Meas.*, vol. 30, no. 7, pp. 573–587, July 2009, doi: 10.1088/0967-3334/30/7/004.

[50] S. Mussnig, S. Krenn, M. Hecking, and P. Wabel, "Assessment of bioimpedance spectroscopy devices: a comparative study and error analysis of gold-plated copper electrodes," *Physiol. Meas.*, vol. 45, no. 2, p. 025001, Feb. 2024, doi: 10.1088/1361-6579/ad205b.

[51] S. Köppä, V. Savolainen, and J. Hyttinen, "Modelling Approach for Assessment of Electrode Configuration and Placement in Bioimpedance Measurements of Skin Irritation," in *5th European Conference of the International Federation for Medical and Biological Engineering*, vol. 37, Á. Jobbágy, Ed., in IFMBE Proceedings, vol. 37., Berlin, Heidelberg: Springer Berlin Heidelberg, 2011, pp. 1238–1241. doi: 10.1007/978-3-642-23508-5_320.

[52] D. W. C. Marcôndes, A. S. Paterno, and P. Bertemes-Filho, "Parasitic Effects on Electrical Bioimpedance Systems: Critical Review," *Sensors*, vol. 22, no. 22, p. 8705, Nov. 2022, doi: 10.3390/s22228705.

[53] L. Nescolarde, H. Lukaski, A. De Lorenzo, B. de-Mateo-Silleras, M. P. Redondo-del-Río, and M. A. Camina-Martín, "Different displacement of bioimpedance vector due to Ag/AgCl electrode effect," *Eur. J. Clin. Nutr.*, vol. 70, no. 12, pp. 1401–1407, Dec. 2016, doi: 10.1038/ejcn.2016.121.

Accepted Manuscript

[54] L. C. Ward, "Bioelectrical impedance analysis for body composition assessment: reflections on accuracy, clinical utility, and standardisation," *Eur. J. Clin. Nutr.*, vol. 73, no. 2, pp. 194–199, Feb. 2019, doi: 10.1038/s41430-018-0335-3.

[55] A. Albulbul, "Evaluating Major Electrode Types for Idle Biological Signal Measurements for Modern Medical Technology," *Bioengineering*, vol. 3, no. 3, p. 20, Aug. 2016, doi: 10.3390/bioengineering3030020.

[56] J. Yao *et al.*, "Development of a Wearable Electrical Impedance Tomographic Sensor for Gesture Recognition with Machine Learning," *IEEE J. Biomed. Health Inform.*, vol. 24, no. 6, pp. 1550–1556, June 2020, doi: 10.1109/JBHI.2019.2945593.

[57] B. Sanchez and S. B. Rutkove, "Electrical Impedance Myography and Its Applications in Neuromuscular Disorders," *Neurotherapeutics*, vol. 14, no. 1, pp. 107–118, Jan. 2017, doi: 10.1007/s13311-016-0491-x.

[58] A. Voropai and V. Sarana, "Low-Noise and Cost-Effective Active Electrodes for Dry Contact ECG Applications," *Sci. Innov.*, vol. 18, no. 1, pp. 112–123, Feb. 2022, doi: 10.15407/scine18.01.112.

[59] A. B. Nigusse, B. Malengier, D. A. Mengistie, A. Maru, and L. Van Langenhove, "Investigating Textile-Based Electrodes for ECG Monitoring in Veterinary Clinical Practice," *AUTEX Res. J.*, vol. 23, no. 4, pp. 551–559, Dec. 2023, doi: 10.2478/aut-2022-0027.

[60] M. Delano, V. Ganapati, R. Kamal, B. Le, J. Le, and R. Mendoza, "Evaluating Research Grade Bioimpedance Hardware Using Textile Electrodes for Long-Term Fluid Status Monitoring," *Front. Electron.*, vol. 2, p. 762442, Jan. 2022, doi: 10.3389/felec.2021.762442.

[61] C.-L. Hu *et al.*, "Dry Wearable Textile Electrodes for Portable Electrical Impedance Tomography," *Sensors*, vol. 21, no. 20, p. 6789, Oct. 2021, doi: 10.3390/s21206789.

[62] S. B. Rutkove, R. A. Partida, G. J. Esper, R. Aaron, and C. A. Shiffman, "Electrode position and size in electrical impedance myography," *Clin. Neurophysiol.*, vol. 116, no. 2, pp. 290–299, Feb. 2005, doi: 10.1016/j.clinph.2004.09.002.

[63] Y. T. Tsukada *et al.*, "Validation of wearable textile electrodes for ECG monitoring," *Heart Vessels*, vol. 34, no. 7, pp. 1203–1211, July 2019, doi: 10.1007/s00380-019-01347-8.

[64] X. An and G. K. Stylios, "A Hybrid Textile Electrode for Electrocardiogram (ECG) Measurement and Motion Tracking," *Materials*, vol. 11, no. 10, p. 1887, Oct. 2018, doi: 10.3390/ma11101887.

[65] T. Alkhidir, A. Sluzek, and M. K. Yapici, "Simple method for adaptive filtering of motion artifacts in E-textile wearable ECG sensors," in *2015 37th Annual International Conference of the IEEE Engineering in Medicine and Biology Society (EMBC)*, Milan: IEEE, Aug. 2015, pp. 3807–3810. doi: 10.1109/EMBC.2015.7319223.

[66] X. An and G. K. Stylios, "Comparison of Motion Artefact Reduction Methods and the Implementation of Adaptive Motion Artefact Reduction in Wearable Electrocardiogram Monitoring," *Sensors*, vol. 20, no. 5, p. 1468, Mar. 2020, doi: 10.3390/s20051468.

[67] X. An, Y. Liu, Y. Zhao, S. Lu, G. K. Stylios, and Q. Liu, "Adaptive Motion Artifact Reduction in Wearable ECG Measurements Using Impedance Pneumography Signal," *Sensors*, vol. 22, no. 15, p. 5493, July 2022, doi: 10.3390/s22155493.

[68] G. Monti, F. Raheli, A. Recupero, and L. Tarricone, "Elastic Textile Wristband for Bioimpedance Measurements," *Sensors*, vol. 23, no. 6, p. 3351, Mar. 2023, doi: 10.3390/s23063351.

[69] G. Cho, K. Jeong, M. J. Paik, Y. Kwun, and M. Sung, "Performance Evaluation of Textile-Based Electrodes and Motion Sensors for Smart Clothing," *IEEE Sens. J.*, vol. 11, no. 12, pp. 3183–3193, Dec. 2011, doi: 10.1109/JSEN.2011.2167508.

[70] K. Wang, D. Zelko, and M. Delano, "Textile band electrodes as an alternative to spot Ag/AgCl electrodes for calf bioimpedance measurements," *Biomed. Phys. Eng. Express*, vol. 6, no. 1, p. 015010, Jan. 2020, doi: 10.1088/2057-1976/ab5b02.

[71] J. Martins *et al.*, "Integrating sEMG and IMU Sensors in an e-Textile Smart Vest for Forward Posture Monitoring: First Steps," *Sensors*, vol. 24, no. 14, p. 4717, July 2024, doi: 10.3390/s24144717.

[72] J. C. Marquez, J. Ferreira, F. Seoane, R. Buendia, and K. Lindecrantz, "Textile electrode straps for wrist-to-ankle bioimpedance measurements for Body Composition Analysis. Initial validation & experimental results," in *2010 Annual International Conference of the IEEE*

Accepted Manuscript

Engineering in Medicine and Biology, Buenos Aires: IEEE, Aug. 2010, pp. 6385–6388. doi: 10.1109/IEMBS.2010.5627305.

[73] Z. Li, Y. Li, M. Liu, L. Cui, and Y. Yu, "Microneedle Electrode Array for Electrical Impedance Myography to Characterize Neurogenic Myopathy," *Ann. Biomed. Eng.*, vol. 44, no. 5, pp. 1566–1575, May 2016, doi: 10.1007/s10439-015-1466-5.

[74] K. Arquilla, A. Webb, and A. Anderson, "Textile Electrocardiogram (ECG) Electrodes for Wearable Health Monitoring," *Sensors*, vol. 20, no. 4, p. 1013, Feb. 2020, doi: 10.3390/s20041013.

[75] X. An, O. Tangsirinaruenart, and G. K. Stylios, "Investigating the performance of dry textile electrodes for wearable end-uses," *J. Text. Inst.*, vol. 110, no. 1, pp. 151–158, Jan. 2019, doi: 10.1080/00405000.2018.1508799.

[76] M. Alizadeh Meghrazi *et al.*, "Multichannel ECG recording from waist using textile sensors," *Biomed. Eng. OnLine*, vol. 19, no. 1, p. 48, Dec. 2020, doi: 10.1186/s12938-020-00788-x.

[77] A. Böhm and B. L. Heitmann, "The use of bioelectrical impedance analysis for body composition in epidemiological studies," *Eur. J. Clin. Nutr.*, vol. 67, no. S1, pp. S79–S85, Jan. 2013, doi: 10.1038/ejcn.2012.168.

[78] H. C. Lukaski, "Evolution of bioimpedance: a circuitous journey from estimation of physiological function to assessment of body composition and a return to clinical research," *Eur. J. Clin. Nutr.*, vol. 67, no. S1, pp. S2–S9, Jan. 2013, doi: 10.1038/ejcn.2012.149.

[79] A. Andreoli, F. Garaci, F. P. Cafarelli, and G. Guglielmi, "Body composition in clinical practice," *Eur. J. Radiol.*, vol. 85, no. 8, pp. 1461–1468, Aug. 2016, doi: 10.1016/j.ejrad.2016.02.005.

[80] H. Sagayama *et al.*, "Comparison of Bioelectrical Impedance Indices for Skeletal Muscle Mass and Intracellular Water Measurements of Physically Active Young Men and Athletes," *J. Nutr.*, vol. 153, no. 9, pp. 2543–2551, Sept. 2023, doi: 10.1016/j.tjnut.2023.07.010.

[81] N. S. D. C. Reis *et al.*, "Agreement of Single-Frequency Electrical Bioimpedance in the Evaluation of Fat Free Mass and Fat Mass in Peritoneal Dialysis Patients," *Front. Nutr.*, vol. 8, p. 686513, May 2021, doi: 10.3389/fnut.2021.686513.

[82] C. N. Matias *et al.*, "Estimation of total body water and extracellular water with bioimpedance in athletes: A need for athlete-specific prediction models," *Clin. Nutr.*, vol. 35, no. 2, pp. 468–474, Apr. 2016, doi: 10.1016/j.clnu.2015.03.013.

[83] U. Kyle, "Bioelectrical impedance analysis?part I: review of principles and methods," *Clin. Nutr.*, vol. 23, no. 5, pp. 1226–1243, Oct. 2004, doi: 10.1016/j.clnu.2004.06.004.

[84] U. G. Kyle *et al.*, "Bioelectrical impedance analysis—part II: utilization in clinical practice," *Clin. Nutr.*, vol. 23, no. 6, pp. 1430–1453, Dec. 2004, doi: 10.1016/j.clnu.2004.09.012.

[85] A. P. Hills and N. M. Byrne, "Bioelectrical impedance and body composition assessment".

[86] R. M. Miller, T. L. Chambers, S. P. Burns, and M. P. Godard, "Validating InBody® 570 Multi-frequency Bioelectrical Impedance Analyzer versus DXA for Body Fat Percentage Analysis.: 3576 Board #15 June 4, 8," *Med. Sci. Sports Exerc.*, vol. 48, p. 991, May 2016, doi: 10.1249/01.mss.0000487979.68551.d7.

[87] C. H. Y. Ling *et al.*, "Accuracy of direct segmental multi-frequency bioimpedance analysis in the assessment of total body and segmental body composition in middle-aged adult population," *Clin. Nutr.*, vol. 30, no. 5, pp. 610–615, Oct. 2011, doi: 10.1016/j.clnu.2011.04.001.

[88] K. Ain, A. P. Putra, O. N. Rahma, D. Hikmawati, A. Rahmatillah, and C. A. C. Abdullah, "Electrical Impedance Spectroscopy as a Potential Tool for Detecting Bone Porosity," *Sens. Actuators Phys.*, vol. 370, p. 115252, May 2024, doi: 10.1016/j.sna.2024.115252.

[89] K. Yokoi, H. C. Lukaski, E. O. Uthus, and F. H. Nielsen, "Use of Bioimpedance Spectroscopy to Estimate Body Water Distribution in Rats Fed High Dietary Sulfur Amino Acids," *J. Nutr.*, vol. 131, no. 4, pp. 1302–1308, Apr. 2001, doi: 10.1093/jn/131.4.1302.

[90] G. Anand and A. Lowe, "Investigating Electrical Impedance Spectroscopy for Estimating Blood Flow-Induced Variations in Human Forearm," *Sensors*, vol. 20, no. 18, p. 5333, Sept. 2020, doi: 10.3390/s20185333.

[91] F. Clemente *et al.*, "Circuital modelling in muscle tissue impedance measurements," *Heliyon*, vol. 10, no. 7, p. e28723, Apr. 2024, doi: 10.1016/j.heliyon.2024.e28723.

Accepted Manuscript

[92] K. J. Wohlgemuth, T. J. Freeborn, K. E. Southall, M. M. Hare, and J. A. Mota, "Can segmental bioelectrical impedance be used as a measure of muscle quality?" *Med. Eng. Phys.*, vol. 124, p. 104103, Feb. 2024, doi: 10.1016/j.medengphy.2024.104103.

[93] S. Eyre, I. Bosaeus, G. Jensen, and A. Saeed, "Using Bioimpedance Spectroscopy for Diagnosis of Malnutrition in Chronic Kidney Disease Stage 5—Is It Useful?" *J. Ren. Nutr.*, vol. 32, no. 2, pp. 170–177, Mar. 2022, doi: 10.1053/j.jrn.2021.03.007.

[94] J. Ferreira, I. Pau, K. Lindecrantz, and F. Seoane, "A Handheld and Textile-Enabled Bioimpedance System for Ubiquitous Body Composition Analysis. An Initial Functional Validation," *IEEE J. Biomed. Health Inform.*, vol. 21, no. 5, pp. 1224–1232, Sept. 2017, doi: 10.1109/JBHI.2016.2628766.

[95] L. Feng, J. Gao, X. Sui, T. Weng, and A. Kong, "Effect of fruit ripeness on electrical impedance spectrum parameters," *LWT*, vol. 208, p. 116751, Sept. 2024, doi: 10.1016/j.lwt.2024.116751.

[96] A. Umehara, T. Oshima, O. S. Deshmukh, T. Nishizu, and T. Imaizumi, "Detection of cell membrane disruption using electrical impedance spectroscopy and acceleration of cell wall modification in carrot processed under low temperature blanching," *J. Food Eng.*, vol. 385, p. 112270, Jan. 2025, doi: 10.1016/j.jfoodeng.2024.112270.

[97] L. Yang, Y. Wu, S. Hu, J. Yao, and F. Chen, "An electrical characteristics extraction and analysis method for the membrane of medaka embryo during its development using electrical impedance spectroscopy," *Bioelectrochemistry*, vol. 163, p. 108885, June 2025, doi: 10.1016/j.bioelechem.2024.108885.

[98] S. Khalil, M. Mohktar, and F. Ibrahim, "The Theory and Fundamentals of Bioimpedance Analysis in Clinical Status Monitoring and Diagnosis of Diseases," *Sensors*, vol. 14, no. 6, pp. 10895–10928, June 2014, doi: 10.3390/s140610895.

[99] R. Kusche and M. Ryschka, "Combining Bioimpedance and EMG Measurements for Reliable Muscle Contraction Detection," *IEEE Sens. J.*, vol. 19, no. 23, pp. 11687–11696, Dec. 2019, doi: 10.1109/JSEN.2019.2936171.

[100] B. Sanchez, O. G. Martinsen, T. J. Freeborn, and C. M. Furse, "Electrical impedance myography: A critical review and outlook," *Clin. Neurophysiol.*, vol. 132, no. 2, pp. 338–344, Feb. 2021, doi: 10.1016/j.clinph.2020.11.014.

[101] C. Hu, T. Wang, K. W. C. Leung, L. Li, and R. K.-Y. Tong, "Muscle Electrical Impedance Properties and Activation Alteration After Functional Electrical Stimulation-Assisted Cycling Training for Chronic Stroke Survivors: A Longitudinal Pilot Study," *Front. Neurol.*, vol. 12, p. 746263, Dec. 2021, doi: 10.3389/fneur.2021.746263.

[102] L. Li, H. Shin, A. Stampas, X. Li, and P. Zhou, "Electrical impedance myography changes after incomplete cervical spinal cord injury: An examination of hand muscles," *Clin. Neurophysiol.*, vol. 128, no. 11, pp. 2242–2247, Nov. 2017, doi: 10.1016/j.clinph.2017.08.027.

[103] S. B. Rutkove, K. S. Lee, C. A. Shiffman, and R. Aaron, "Test–retest reproducibility of 50kHz linear-electrical impedance myography," *Clin. Neurophysiol.*, vol. 117, no. 6, pp. 1244–1248, June 2006, doi: 10.1016/j.clinph.2005.12.029.

[104] M. Jafarpoor, Jia Li, J. K. White, and S. B. Rutkove, "Optimizing Electrode Configuration for Electrical Impedance Measurements of Muscle via the Finite Element Method," *IEEE Trans. Biomed. Eng.*, vol. 60, no. 5, pp. 1446–1452, May 2013, doi: 10.1109/TBME.2012.2237030.

[105] S. Baidya and M. A. Ahad, "Assessment of Optimized Electrode Configuration for Electrical Impedance Myography Using Genetic Algorithm via Finite Element Model," *J. Med. Eng.*, vol. 2016, pp. 1–7, Oct. 2016, doi: 10.1155/2016/9123464.

[106] S. B. Rutkove, A. Pacheck, and B. Sanchez, "Sensitivity distribution simulations of surface electrode configurations for electrical impedance myography," *Muscle Nerve*, vol. 56, no. 5, pp. 887–895, Nov. 2017, doi: 10.1002/mus.25561.

[107] S. B. Rutkove, "Electrical impedance myography: Background, current state, and future directions," *Muscle Nerve*, vol. 40, no. 6, pp. 936–946, Dec. 2009, doi: 10.1002/mus.21362.

[108] S. Schwartz, T. R. Geisbush, A. Mijailovic, A. Pasternak, B. T. Darras, and S. B. Rutkove, "Optimizing electrical impedance myography measurements by using a multifrequency ratio: A study in Duchenne muscular dystrophy," *Clin. Neurophysiol.*, vol. 126, no. 1, pp. 202–208, Jan. 2015, doi: 10.1016/j.clinph.2014.05.007.

Accepted Manuscript

[109] Z. Wei *et al.*, "A Time-Frequency Measurement and Evaluation Approach for Body Channel Characteristics in Galvanic Coupling Intrabody Communication," *Sensors*, vol. 21, no. 2, p. 348, Jan. 2021, doi: 10.3390/s21020348.

[110] Keysight, "E4990A Impedance Analyzer, 20 Hz to 10/20/30/50/120 MHz," Keysight. Accessed: May 22, 2025. [Online]. Available: https://www.keysight.com/us/en/product/E4990A/impedance-analyzer-20-hz-10-20-30-50-120-mhz.html

[111] "SFB7 BIS Research Device | ImpediMed." Accessed: May 22, 2025. [Online]. Available: https://www.impedimed.com/products/research-devices/sfb7/

[112] B. Sanchez, C. R. Rojas, G. Vandersteen, R. Bragos, and J. Schoukens, "On the calculation of the *D* -optimal multisine excitation power spectrum for broadband impedance spectroscopy measurements," *Meas. Sci. Technol.*, vol. 23, no. 8, p. 085702, Aug. 2012, doi: 10.1088/0957-0233/23/8/085702.

[113] W. Wang, Y. Tang, X. Zhang, and K. Wang, "Design of a recursive single-bin DFT algorithm for sparse spectrum analysis," *Clust. Comput.*, vol. 20, no. 2, pp. 1483–1492, June 2017, doi: 10.1007/s10586-017-0866-8.

[114] R. Nie, N. Abimbola Sunmonu, A. B. Chin, K. S. Lee, and S. B. Rutkove, "Electrical impedance myography: Transitioning from human to animal studies," *Clin. Neurophysiol.*, vol. 117, no. 8, pp. 1844–1849, Aug. 2006, doi: 10.1016/j.clinph.2006.03.024.

[115] J. Zhu *et al.*, "EIT-kit: An Electrical Impedance Tomography Toolkit for Health and Motion Sensing," in *The 34th Annual ACM Symposium on User Interface Software and Technology*, Virtual Event USA: ACM, Oct. 2021, pp. 400–413. doi: 10.1145/3472749.3474758.

[116] M. Cheney, D. Isaacson, and J. C. Newell, "Electrical Impedance Tomography".

[117] L. Youssef Baby, R. S. Bedran, A. Doumit, R. H. El Hassan, and N. Maalouf, "Past, present, and future of electrical impedance tomography and myography for medical applications: a scoping review," *Front. Bioeng. Biotechnol.*, vol. 12, p. 1486789, Dec. 2024, doi: 10.3389/fbioe.2024.1486789.

[118] M. Vauhkonen, P. A. Karjalainen, and J. P. Kaipio, "A Kalman filter approach to track fast impedance changes in electrical impedance tomography," *IEEE Trans. Biomed. Eng.*, vol. 45, no. 4, pp. 486–493, Apr. 1998, doi: 10.1109/10.664204.

[119] A. Adler and A. Boyle, "Electrical Impedance Tomography: Tissue Properties to Image Measures," *IEEE Trans. Biomed. Eng.*, vol. 64, no. 11, pp. 2494–2504, Nov. 2017, doi: 10.1109/TBME.2017.2728323.

[120] S. Mansouri, Y. Alharbi, F. Haddad, S. Chabcoub, A. Alshrouf, and A. A. Abd-Elghany, "Electrical Impedance tomography – recent applications and developments," *J. Electr. Bioimpedance*, vol. 12, no. 1, pp. 50–62, Jan. 2021, doi: 10.2478/joeb-2021-0007.

[121] D. P. Leins, C. Gibas, R. Brück, and R. Haschke, "Toward More Robust Hand Gesture Recognition on EIT Data," *Front. Neurorobotics*, vol. 15, p. 659311, Aug. 2021, doi: 10.3389/fnbot.2021.659311.

[122] C. Wang *et al.*, "Flexi-EIT: A Flexible and Reconfigurable Active Electrode Electrical Impedance Tomography System," *IEEE Trans. Biomed. Circuits Syst.*, vol. 18, no. 1, pp. 89–99, Feb. 2024, doi: 10.1109/TBCAS.2023.3307500.

[123] D. Jiang, Y. Wu, and A. Demosthenous, "Hand Gesture Recognition Using Three-Dimensional Electrical Impedance Tomography," *IEEE Trans. Circuits Syst. II Express Briefs*, vol. 67, no. 9, pp. 1554–1558, Sept. 2020, doi: 10.1109/TCSII.2020.3006430.

[124] Z. Hao, S. Yue, B. Sun, and H. Wang, "Optimal distance of multi-plane sensor in three-dimensional electrical impedance tomography," *Comput. Assist. Surg.*, vol. 22, no. sup1, pp. 326–338, Oct. 2017, doi: 10.1080/24699322.2017.1389412.

[125] B. Schullcke, B. Gong, S. Krueger-Ziolek, and K. Moeller, "Reconstruction of conductivity change in lung lobes utilizing electrical impedance tomography," *Curr. Dir. Biomed. Eng.*, vol. 3, no. 2, pp. 513–516, Sept. 2017, doi: 10.1515/cdbme-2017-0108.

[126] M. Soleimani, C. Gómez-Laberge, and A. Adler, "Imaging of conductivity changes and electrode movement in EIT," *Physiol. Meas.*, vol. 27, no. 5, pp. S103–S113, May 2006, doi: 10.1088/0967-3334/27/5/S09.

Accepted Manuscript

[127] Y. Li *et al.*, "Robust electrical impedance tomography for biological application: A mini review," *Heliyon*, vol. 9, no. 4, p. e15195, Apr. 2023, doi: 10.1016/j.heliyon.2023.e15195.
[128] L. Youssef Baby, R. S. Bedran, A. Doumit, R. H. El Hassan, and N. Maalouf, "Past, present, and future of electrical impedance tomography and myography for medical applications: a scoping review," *Front. Bioeng. Biotechnol.*, vol. 12, p. 1486789, Dec. 2024, doi: 10.3389/fbioe.2024.1486789.
[129] T. Zhang *et al.*, "Advances of deep learning in electrical impedance tomography image reconstruction," *Front. Bioeng. Biotechnol.*, vol. 10, p. 1019531, Dec. 2022, doi: 10.3389/fbioe.2022.1019531.
[130] I. Cappellini, L. Campagnola, and G. Consales, "Electrical Impedance Tomography, Artificial Intelligence, and Variable Ventilation: Transforming Respiratory Monitoring and Treatment in Critical Care," *J. Pers. Med.*, vol. 14, no. 7, p. 677, June 2024, doi: 10.3390/jpm14070677.
[131] P. J. Vauhkonen, M. Vauhkonen, T. Mäkinen, P. A. Karjalainen, and J. P. Kaipio, "Dynamic electrical impedance tomography - phantom studies," *Inverse Probl. Eng.*, vol. 8, no. 5, pp. 495–510, Oct. 2000, doi: 10.1080/174159700088027743.
[132] K. Y. Kim, S. I. Kang, M. C. Kim, S. Kim, Y. J. Lee, and M. Vauhkonen, "Dynamic Electrical Impedance Tomography with Known Internal Structures," *Inverse Probl. Eng.*, vol. 11, no. 1, pp. 1–19, Jan. 2003, doi: 10.1080/1068276021000014705.
[133] A. Adler, "EIDORS." Accessed: May 14, 2025. [Online]. Available: https://www.sce.carleton.ca/faculty/adler/eidors/tutorial/EIDORS_basics/tutorial010.shtml
[134] P. N. Darma and M. Takei, "High-Speed and Accurate Meat Composition Imaging by Mechanically-Flexible Electrical Impedance Tomography With *k* -Nearest Neighbor and Fuzzy *k* -Means Machine Learning Approaches," *IEEE Access*, vol. 9, pp. 38792–38801, 2021, doi: 10.1109/ACCESS.2021.3064315.
[135] D. Pessoa *et al.*, "Classification of Electrical Impedance Tomography Data Using Machine Learning," Aug. 02, 2021, *arXiv*: arXiv:2108.01668. doi: 10.48550/arXiv.2108.01668.
[136] X. Lu, S. Sun, K. Liu, J. Sun, and L. Xu, "Development of a Wearable Gesture Recognition System Based on Two-Terminal Electrical Impedance Tomography," *IEEE J. Biomed. Health Inform.*, vol. 26, no. 6, pp. 2515–2523, June 2022, doi: 10.1109/JBHI.2021.3130374.
[137] A. Bailleul *et al.*, "Bioimpedance Spectroscopy Helps Monitor the Impact of Electrical Stimulation on Muscle Cells," *IEEE Access*, vol. 10, pp. 131430–131441, 2022, doi: 10.1109/ACCESS.2022.3228479.
[138] A. Hafid, S. Zolfaghari, A. Kristoffersson, and M. Folke, "Exploring the potential of electrical bioimpedance technique for analyzing physical activity," *Front. Physiol.*, vol. 15, p. 1515431, Dec. 2024, doi: 10.3389/fphys.2024.1515431.
[139] R. Kusche, A. Oltmann, and P. Rostalski, "A Wearable Dual-Channel Bioimpedance Spectrometer for Real-Time Muscle Contraction Detection," *IEEE Sens. J.*, vol. 24, no. 7, pp. 11316–11327, Apr. 2024, doi: 10.1109/JSEN.2024.3359284.
[140] Smita Patil, "Electrical Impedance Tomography for Real-Time Monitoring of Muscle Activity in Robot-Assisted Rehabilitation," *J. Electr. Syst.*, vol. 20, no. 1s, pp. 1036–1047, Mar. 2024, doi: 10.52783/jes.871.
[141] Z. Gong, W. L. A. Lo, R. Wang, and L. Li, "Electrical impedance myography combined with quantitative assessment techniques in paretic muscle of stroke survivors: Insights and challenges," *Front. Aging Neurosci.*, vol. 15, p. 1130230, Mar. 2023, doi: 10.3389/fnagi.2023.1130230.
[142] L. Li, A. Stampas, H. Shin, X. Li, and P. Zhou, "Alterations in Localized Electrical Impedance Myography of Biceps Brachii Muscles Paralyzed by Spinal Cord Injury," *Front. Neurol.*, vol. 8, p. 253, June 2017, doi: 10.3389/fneur.2017.00253.
[143] G. C. Ozmen *et al.*, "Mid-Activity and At-Home Wearable Bioimpedance Elucidates an Interpretable Digital Biomarker of Muscle Fatigue," *IEEE Trans. Biomed. Eng.*, vol. 70, no. 12, pp. 3513–3524, Dec. 2023, doi: 10.1109/TBME.2023.3290530.
[144] G. Vescio, J. Rosell, L. Nescolarde, and G. Giovinazzo, "Muscle Fatigue Monitoring Using a Multifrequency Bioimpedance Technique," in *5th European Conference of the International Federation for Medical and Biological Engineering*, vol. 37, Á. Jobbágy, Ed., in IFMBE

Accepted Manuscript

Proceedings, vol. 37. , Berlin, Heidelberg: Springer Berlin Heidelberg, 2011, pp. 1257–1260. doi: 10.1007/978-3-642-23508-5_325.

[145] S. Yamaguchi *et al.*, "Bioimpedance analysis for identifying new indicators of exercise-induced muscle damage," *Sci. Rep.*, vol. 14, no. 1, p. 15299, July 2024, doi: 10.1038/s41598-024-66089-8.

[146] L. K. Huang, L. N. Huang, Y. M. Gao, Z. Lucev Vasic, M. Cifrek, and M. Du, "Electrical Impedance Myography Applied to Monitoring of Muscle Fatigue During Dynamic Contractions," *IEEE Access*, vol. 8, pp. 13056–13065, 2020, doi: 10.1109/ACCESS.2020.2965982.

[147] T. J. Freeborn and B. Fu, "Time-course bicep tissue bio-impedance changes throughout a fatiguing exercise protocol," *Med. Eng. Phys.*, vol. 69, pp. 109–115, July 2019, doi: 10.1016/j.medengphy.2019.04.006.

[148] T. J. Freeborn, G. Regard, and B. Fu, "Localized Bicep Tissue Bioimpedance Alterations Following Eccentric Exercise in Healthy Young Adults," *IEEE Access*, vol. 8, pp. 23100–23109, 2020, doi: 10.1109/ACCESS.2020.2970314.

[149] B. Zhou *et al.*, "Electrical Impedance Myography for Evaluating Muscle Fatigue Induced by Neuromuscular Electrical Stimulation," *IEEE J. Electromagn. RF Microw. Med. Biol.*, vol. 6, no. 1, pp. 94–102, Mar. 2022, doi: 10.1109/JERM.2021.3092883.

[150] T. J. Freeborn and B. Fu, "Fatigue-Induced Cole Electrical Impedance Model Changes of Biceps Tissue Bioimpedance," *Fractal Fract.*, vol. 2, no. 4, p. 27, Oct. 2018, doi: 10.3390/fractalfract2040027.

[151] L. Li, H. Shin, X. Li, S. Li, and P. Zhou, "Localized Electrical Impedance Myography of the Biceps Brachii Muscle during Different Levels of Isometric Contraction and Fatigue," *Sensors*, vol. 16, no. 4, p. 581, Apr. 2016, doi: 10.3390/s16040581.

[152] R. Kusche and M. Ryschka, "Multi-Frequency Impedance Myography: The PhaseX Effect," *IEEE Sens. J.*, vol. 21, no. 3, pp. 3791–3798, Feb. 2021, doi: 10.1109/JSEN.2020.3022899.

[153] M. Y. Yakim, A. V. Kobelev, and S. I. Shchukin, "Real-Time Signal Processing for Muscle Contraction Detection Based on Electrical Impedance Measurements," in *2024 IEEE 3rd International Conference on Problems of Informatics, Electronics and Radio Engineering (PIERE)*, Novosibirsk, Russian Federation: IEEE, Nov. 2024, pp. 580–583. doi: 10.1109/PIERE62470.2024.10804964.

[154] N. Vaquero-Gallardo and H. Martínez-García, "Electrical Impedance Tomography for Hand Gesture Recognition for HMI Interaction Applications," *J. Low Power Electron. Appl.*, vol. 12, no. 3, p. 41, July 2022, doi: 10.3390/jlpea12030041.

[155] C. Gibas, A. Grunewald, H.-W. Wunderlich, P. Marx, and R. Bruck, "A wearable EIT system for detection of muscular activity in the extremities," in *2019 41st Annual International Conference of the IEEE Engineering in Medicine and Biology Society (EMBC)*, Berlin, Germany: IEEE, July 2019, pp. 2496–2499. doi: 10.1109/EMBC.2019.8856792.

[156] B. Sanchez and S. B. Rutkove, "Present Uses, Future Applications, and Technical Underpinnings of Electrical Impedance Myography," *Curr. Neurol. Neurosci. Rep.*, vol. 17, no. 11, p. 86, Nov. 2017, doi: 10.1007/s11910-017-0793-3.

[157] S. B. Rutkove and B. Sanchez, "Electrical Impedance Methods in Neuromuscular Assessment: An Overview," *Cold Spring Harb. Perspect. Med.*, vol. 9, no. 10, p. a034405, Oct. 2019, doi: 10.1101/cshperspect.a034405.

[158] J. J. P. Alix *et al.*, "Multi-dimensional electrical impedance myography of the tongue as a potential biomarker for amyotrophic lateral sclerosis," *Clin. Neurophysiol.*, vol. 131, no. 4, pp. 799–808, Apr. 2020, doi: 10.1016/j.clinph.2019.12.418.

[159] L. D. Hobson-Webb, P. J. Zwelling, S. S. Raja, A. N. Pifer, and P. S. Kishnani, "Quantitative muscle ultrasound and electrical impedance myography in late onset Pompe disease: A pilot study of reliability, longitudinal change and correlation with function," *Mol. Genet. Metab. Rep.*, vol. 28, p. 100785, Sept. 2021, doi: 10.1016/j.ymgmr.2021.100785.

[160] B. Sanchez *et al.*, "Non-invasive assessment of muscle injury in healthy and dystrophic animals with electrical impedance myography," *Muscle Nerve*, vol. 56, no. 6, Dec. 2017, doi: 10.1002/mus.25559.

Accepted Manuscript

[161] F. Alvarado-Arriagada, B. Fernández-Arroyo, S. Rebolledo, and E. J. Pino, "Development and Validation of a Portable EIT System for Real-Time Respiratory Monitoring," *Sensors*, vol. 24, no. 20, p. 6642, Oct. 2024, doi: 10.3390/s24206642.

[162] B. Schullcke *et al.*, "Lobe based image reconstruction in Electrical Impedance Tomography," *Med. Phys.*, vol. 44, no. 2, pp. 426–436, Feb. 2017, doi: 10.1002/mp.12038.

[163] G. Hornero, D. Díaz, and O. Casas, "Bioimpedance system for monitoring muscle and cardiovascular activity in the stump of lower-limb amputees," *Physiol. Meas.*, vol. 34, no. 2, pp. 189–201, Feb. 2013, doi: 10.1088/0967-3334/34/2/189.

[164] S. Boyas and A. Guével, "Neuromuscular fatigue in healthy muscle: Underlying factors and adaptation mechanisms," *Ann. Phys. Rehabil. Med.*, vol. 54, no. 2, pp. 88–108, Mar. 2011, doi: 10.1016/j.rehab.2011.01.001.

[165] C. A. Shiffman, R. Aaron, and S. B. Rutkove, "Electrical impedance of muscle during isometric contraction," *Physiol. Meas.*, vol. 24, no. 1, pp. 213–234, Feb. 2003, doi: 10.1088/0967-3334/24/1/316.

[166] B. Ben Atitallah *et al.*, "Hand Sign Recognition System Based on EIT Imaging and Robust CNN Classification," *IEEE Sens. J.*, vol. 22, no. 2, pp. 1729–1737, Jan. 2022, doi: 10.1109/JSEN.2021.3130982.

[167] M. Mortreux, C. Semple, D. Riveros, J. A. Nagy, and S. B. Rutkove, "Electrical impedance myography for the detection of muscle inflammation induced by λ-carrageenan," *PLOS ONE*, vol. 14, no. 10, p. e0223265, Oct. 2019, doi: 10.1371/journal.pone.0223265.

[168] Á. Cebrián-Ponce, A. Irurtia, M. Carrasco-Marginet, G. Saco-Ledo, M. Girabent-Farrés, and J. Castizo-Olier, "Electrical Impedance Myography in Health and Physical Exercise: A Systematic Review and Future Perspectives," *Front. Physiol.*, vol. 12, p. 740877, Sept. 2021, doi: 10.3389/fphys.2021.740877.

[169] M. E. Rosa-Caldwell, S. Pandeya, M. Mortreux, and S. B. Rutkove, "Predicting muscle function and mass with electrical impedance myography: A study in rat analogs of micro- and partial gravity," *Acta Astronaut.*, vol. 223, pp. 384–388, Oct. 2024, doi: 10.1016/j.actaastro.2024.07.017.

[170] S. B. Rutkove *et al.*, "Electrical impedance myography detects age-related skeletal muscle atrophy in adult zebrafish," *Sci. Rep.*, vol. 13, no. 1, p. 7191, May 2023, doi: 10.1038/s41598-023-34119-6.

[171] I. Costanzo, D. Sen, L. Rhein, and U. Guler, "Respiratory Monitoring: Current State of the Art and Future Roads," *IEEE Rev. Biomed. Eng.*, vol. 15, pp. 103–121, 2022, doi: 10.1109/RBME.2020.3036330.

[172] L. Sang, Z. Zhao, Z. Lin, X. Liu, N. Zhong, and Y. Li, "A narrative review of electrical impedance tomography in lung diseases with flow limitation and hyperinflation: methodologies and applications," *Ann. Transl. Med.*, vol. 8, no. 24, pp. 1688–1688, Dec. 2020, doi: 10.21037/atm-20-4984.

[173] M. Cheney, D. Isaacson, J. C. Newell, S. Simske, and J. Goble, "NOSER: An algorithm for solving the inverse conductivity problem," *Int. J. Imaging Syst. Technol.*, vol. 2, no. 2, pp. 66–75, June 1990, doi: 10.1002/ima.1850020203.

[174] L. Plantagie and K. J. Batenburg, "Approximating Algebraic Tomography Methods by Filtered Backprojection: A Local Filter Approach," *Fundam. Informaticae*, vol. 135, no. 1–2, pp. 1–19, 2014, doi: 10.3233/FI-2014-1109.

[175] E. J. Woo and J. K. Seo, "Magnetic resonance electrical impedance tomography (MREIT) for high-resolution conductivity imaging," *Physiol. Meas.*, vol. 29, no. 10, pp. R1–R26, Oct. 2008, doi: 10.1088/0967-3334/29/10/R01.

[176] J. N. Wang *et al.*, "Optimization of the electrode configuration of electrical impedance myography for wearable application," *Automatika*, vol. 61, no. 3, pp. 475–481, July 2020, doi: 10.1080/00051144.2020.1783615.

[177] B. Sanchez, A. Pacheck, and S. B. Rutkove, "Guidelines to electrode positioning for human and animal electrical impedance myography research," *Sci. Rep.*, vol. 6, no. 1, p. 32615, Sept. 2016, doi: 10.1038/srep32615.

Accepted Manuscript

[178] H. Kwon, J. F. Di Cristina, S. B. Rutkove, and B. Sanchez, "Recording characteristics of electrical impedance-electromyography needle electrodes," *Physiol. Meas.*, vol. 39, no. 5, p. 055005, May 2018, doi: 10.1088/1361-6579/aabb8c.

[179] M. Soleimani, "Electrical impedance tomography imaging using a priori ultrasound data," *Biomed. Eng. OnLine*, vol. 5, no. 1, p. 8, Dec. 2006, doi: 10.1186/1475-925X-5-8.

[180] E. K. Murphy, J. Skinner, M. Martucci, S. B. Rutkove, and R. J. Halter, "Toward Electrical Impedance Tomography Coupled Ultrasound Imaging for Assessing Muscle Health," *IEEE Trans. Med. Imaging*, vol. 38, no. 6, pp. 1409–1419, June 2019, doi: 10.1109/TMI.2018.2886152.

[181] C. Ngo *et al.*, "A Wearable, Multi-Frequency Device to Measure Muscle Activity Combining Simultaneous Electromyography and Electrical Impedance Myography," *Sensors*, vol. 22, no. 5, p. 1941, Mar. 2022, doi: 10.3390/s22051941.

[182] M. Liu, V. F. Rey, Y. Zhang, L. S. S. Ray, B. Zhou, and P. Lukowicz, "iMove: Exploring Bio-impedance Sensing for Fitness Activity Recognition," in *2024 IEEE International Conference on Pervasive Computing and Communications (PerCom)*, Mar. 2024, pp. 194–205. doi: 10.1109/PerCom59722.2024.10494489.

[183] M. H. Jung *et al.*, "Wrist-wearable bioelectrical impedance analyzer with miniature electrodes for daily obesity management," *Sci. Rep.*, vol. 11, no. 1, p. 1238, Jan. 2021, doi: 10.1038/s41598-020-79667-3.

[184] M. Usman, A. K. Gupta, and W. Xue, "Wearable ring bioelectrical impedance analyzer for estimation and monitoring of body fat," *Smart Health*, vol. 24, p. 100275, June 2022, doi: 10.1016/j.smhl.2022.100275.

[185] H. Dong, S. Teng, X. Wu, X. Han, F. Giorgio-Serchi, and Y. Yang, "Flexible electrical impedance tomography for tactile interfaces," Nov. 20, 2024, *arXiv*: arXiv:2411.13306. doi: 10.48550/arXiv.2411.13306.

[186] C. Cornelius, R. Peterson, J. Skinner, R. Halter, and D. Kotz, "A wearable system that knows who wears it," in *Proceedings of the 12th annual international conference on Mobile systems, applications, and services*, Bretton Woods New Hampshire USA: ACM, June 2014, pp. 55–67. doi: 10.1145/2594368.2594369.

[187] S. Rossi, C. Mancarella, C. Mocenni, and L. Della Torre, "Bioimpedance sensing in wearable systems: From hardware integration to model development," in *2017 IEEE 3rd International Forum on Research and Technologies for Society and Industry (RTSI)*, Modena, Italy: IEEE, Sept. 2017, pp. 1–6. doi: 10.1109/RTSI.2017.8065956.

[188] S. F. Scagliusi *et al.*, "Wearable Devices Based on Bioimpedance Test in Heart-Failure: Design Issues," *Rev. Cardiovasc. Med.*, vol. 25, no. 9, p. 320, Sept. 2024, doi: 10.31083/j.rcm2509320.

Accepted Manuscript